In Vitro Pharmacological Inhibition of Myofibroblast Differentiation and Force Generation in a Collagen-GAG Matrix

by

Eric C. Soller
B.S., Mechanical Engineering
Rose-Hulman Institute of Technology, 2003

Submitted to the Department of Mechanical Engineering in Partial Fulfillment of the Requirements for the Degree of

Master of Science in Mechanical Engineering

at the
Massachusetts Institute of Technology
June, 2005

Signature of Author_____
Department of Mechanical Engineering
May 20, 2005

Certified by_____
Ioannis V. Yannas
Professor of Mechanical and Biological Engineering
Thesis Supervisor

Accepted by_____
Lallit Anand
Professor of Mechanical Engineering
Chairman, Department Committee on Graduate Students

In Vitro Pharmacological Inhibition of Myofibroblast Differentiation and Force Generation in a Collagen-GAG Matrix

by

Eric C. Soller

Submitted to the Department of Mechanical Engineering
on May 20, 2005 in Partial Fulfillment of the
Requirements for the Degree of
Master of Science in Mechanical Engineering

ABSTRACT

Induced regeneration studies from three organs in the adult mammal (skin, peripheral nerves, and the conjunctiva) suggest an antagonistic relationship between myofibroblast-mediated contraction of wounds and induced regeneration. In each instance of induced regeneration, contraction blocking was accomplished using regeneration templates, or scaffolds of highly specific structural and chemical properties that mainly control the environment or the density of contractile cells (myofibroblasts). In addition to scaffolds, diffusible factors could be used to inhibit specific components of the intracellular pathway in an effort to further evaluate the relationship between contraction and induced regeneration. The crucial role that Rho-associated coiled-coil forming protein serine/threonine kinase (ROCK) seems to play in cell-mediated contraction and cytoskeletal remodeling behavior of fibroblasts make it an attractive target for pharmacological inhibition.

A preliminary *in vitro* study was conducted to evaluate the effect of Y-27632, a specific pharmacological inhibitor of ROCK, on the contraction of highly porous, three-dimensional type I collagen-glycosaminoglycan (CG) matrices over time by attached NR6WT fibroblasts treated with TGF-β1, a known upregulator of both fibroblast contraction and expression of the contractile filament α-smooth muscle actin (α-SMA), a hallmark of the myofibroblast phenotype.

NR6WT fibroblasts were seeded into free-floating cylindrical CG matrices (8 mm in diameter, n=6) and treated with serum-containing media supplemented with TGF-β1 (3 ng/ml) or both TGF-β1 (3 ng/ml) and Y-27632 (10 μM) for 12 days. Control cells (untreated) were cultured as well as unseeded matrix controls. The diameter reduction of matrices was determined daily by visual comparison to circles of known diameter (± .5 mm). Contraction was calculated as the change in matrix diameter from the day 0 value divided by the day 0 diameter and is a measure of radial strain in the substrate. Cell-mediated contraction (CMC) was determined by subtracting the contraction of the unseeded matrices from the contraction of the seeded matrices. The average number of attached fibroblasts per matrix for each experimental group was determined at the end of the 12 day contraction experiment.

At a dosage of 10 μM, Y-27632 significantly attenuated TGF-β1-stimulated cell-mediated contraction of free-floating CG matrices by NR6WT fibroblasts. While Y-27632 treatment also decreased the cellular content of the matrices compared to control cells, the relative magnitudes of cell-mediated contraction (CMC) normalized to the attached number of fibroblasts indicate a statistically significant difference between mean values for TGF-β1 treated cells and cells treated with both TGF-β1 and Y-27632 ($p<0.001$). The data suggest that cellular de-adhesion alone does not account for the inhibitory effect of Y-27632 on TGF-β1 stimulated cell-mediated contraction of CG matrices. A likely explanation is that the inhibitor is blocking the ability of fibroblasts to express an agonist-induced contractile phenotype and instead encouraging the development of a more migratory one. The observed effect of the inhibitor on contraction could have been through inhibition of the contractile filament α-SMA, although expression of this protein was not assayed in this study.

The demonstrated ability of Y-27632 to inhibit TGF-β1-stimulated force generation support its use in a future *in vivo* study that would evaluate the relationship between contraction blocking using pharmacological inhibitors and induced regeneration in a peripheral nerve wound model.

Thesis Supervisor: Ioannis V. Yannas
Title: Professor of Mechanical and Biological Engineering

Acknowledgements

Looking back on my graduate experience, I have many to thank for where I stand today. First and foremost, I am grateful to Professor Ioannis Yannas for appointing me to the Fibers and Polymers Laboratory. I have learned much from you in two years and thrived under your mentorship as a developing scientist, teacher, and graduate student. Thank you for your constant guidance and encouragement. I have enjoyed our frequent conversations, not only on all things research, but also on another issue of critical importance: the status of the Red Sox starting nine.

I am grateful to Professor Myron Spector for his central role in my education as well as his generous support and enthusiasm. In addition, I am indebted to Professor Lorna Gibson for the gracious use of her laboratory facilities.

I would like to thank both past and present members of the Fibers and Polymers (FPL), Orthopaedic Research Lab (ORL) and Cellular Solids Group at MIT.

I am particularly indebted to Karolina Corin, my collaborator and partner-in-crime. As life alarmingly began to resemble the Piled Higher and Deeper (PhD) comic strip, I thank you for your compassion and hard work along the way. As you well know, this work would not have been possible without you.

I praise the patience of Andrew Albers as I got my feet wet in the wonderful world of cell culture and animal tissue harvesting. While it is said that there are no stupid questions, thank you for calmly responding to many of mine with a subtle, amused-yet-not-quite-condescending look. I have added it to my repertoire and it has served me well with my own students.

Brendan Harley must be commended for selflessly sharing both his expertise in the laboratory and his boundless knowledge of just about everything. You have been an incredible resource and mentor along the way.

Barring the time on my 16th birthday when they led me blindfolded to our driveway to receive a new lawnmower (instead of a car), my mother and father have been wonderful parents. From an early age you encouraged me to strive to know myself and my strengths and to make the most of the natural gifts that I've been given. Thank you for reminding me that much is required of me and guiding me to find value in life based on the contributions that I make.

I thank my four brothers for the great fun I had growing up and continue to have when we are together. Thanks for making it impossible for me to take myself too seriously. In many ways I owe my sense of self (and humor) to all of you.

On the plains of Central Texas it was my grandfather, James Camillo Flanagan, P.E., who first taught me to appreciate my mind and to approach the world around me in a sensible and analytical manner. You will always have my utmost respect and admiration.

To the many friends who have made my life in Boston over the past two years both eventful and something very special – I thank you.

Finally, while I am not ready to forgive the 2003 Boston Red Sox for breaking my heart, I would like to thank the 2004 squad for having the good sense to wait until I moved to this city before winning it all.

Table of Contents

List of Figures

List of Tables

Chapter 1. Introduction and Background

1.1 Macroscopic Outcomes of Spontaneous Healing: Repair vs. Regeneration

Acute or chronic injury to an organ is followed by a spontaneous healing process. During the early stages of gestation, injury to the mammalian fetus is reversible. During this period the spontaneous wound response is capable of restoring the structure and function of the original organ, a process called *regeneration*. In contrast, the unimpaired response of adults to severe injury is an irreversible process leading to closure of the injured site by contraction and formation of scar, a non-physiological tissue (*repair*). The consequences of irreversible healing at the organ scale are far-reaching: they often result in an essentially nonfunctional organ.

There is accumulating evidence that the spontaneous healing process of an injured organ in the adult mammal can be modified to yield a partially or completely regenerated organ. Regenerative medicine is an emerging field of study involving the implantation of biomaterials to facilitate formation (regeneration) of tissue *in vivo*. This field is undergoing rapid growth at this time, as evidenced by observation of regeneration or reported progress in on-going research efforts in a wide range of organs including skin [5], conjunctiva [6], peripheral nerves [7], bone [8], heart valves [9], articular cartilage [10], urological organs [11], and the spinal cord [12].

The basic outline of a hypothetical mechanism for induced organ regeneration has become clear. It relies on regenerative studies in three organs (skin, conjunctiva and peripheral nerves), which started much earlier and have progressed much further than research in other organs. From these studies a pattern has emerged, based on two observations: i) regeneration was successfully induced, at least partially, when contraction was blocked, following grafting with a class of scaffolds (collectively referred to as "regeneration templates") that were characterized by a very highly specific structure (chemical composition, pore size, degradation rate, pore volume fraction) and ii) when a class of "inactive scaffolds" with slightly different properties than their biologically active counterparts was used, regeneration was thwarted and vigorous contraction ensued. The available data support the hypothesis of contraction blocking as a plausible mechanism for induced organ regeneration in the adult mammal. In almost all such processes the critical reactant supplied by the investigators was a scaffold, a highly porous, degradable macromolecular solid that has a specific contraction-blocking activity as well as the ability to mimic the *in vivo* environment, and particularly the stroma, of the organ.

1.2 Repair: Mechanism of Contraction

Similarities in the mechanistic hypotheses for inducing regeneration of skin and peripheral nerves originate in their common response to irreversible injury. Both organs spontaneously respond to injury by recruiting contractile cells that, if not properly suppressed, drive closure of the defect by contraction and scar synthesis rather than by regeneration. Contraction of skin defects starts from a cell cluster at the edge of the defect (forming what is referred to as a "picture frame" model) that will later move inward, decreasing the defect area. In peripheral nerves, contraction primarily results from the activity of a circumstantial sheath of contractile cells.

The well-documented, macroscopic contraction that drives the closure of skin defects finds its origin at the cellular scale, arising from the individual contribution of contractile forces generated by differentiated myofibroblasts [13-15]. The current consensus is that myofibroblasts (MFB) present in the granulation tissue following skin wounding derive directly from fibroblasts and comprise an intermediate, contractile, cellular phenotype between the fibroblast and the smooth muscle cell [14]. There is also evidence that undifferentiated fibroblasts may contribute to macroscopic contraction by applying traction to the ECM very soon after coming into contact with it [16-20].

In response to external tension, fibroblasts exert what appears to be a sustained, approximately isometric force on their surrounding environment via a Rho/Rho-kinase (ROCK)-mediated, actomyosin contractile apparatus[21-23]. This three-dimensional, transcellular structure consists of bundles of actin and non-muscle myosin microfilaments called 'stress fibers.'

Of the many ultrastructural and biochemical factors that distinguish myofibroblasts from their fibroblast precursors, the most useful operational distinction of MFB differentiation is expression of the α-smooth muscle actin (α-SMA) phenotype [13-15]. Stress fibers of immature myofibroblasts (called proto-myofibroblasts) contain only beta- and gamma-cytoplasmic actins [14]. Additionally, differentiated myofibroblasts exhibit stress fibers typically arranged parallel to the long axis of the cell, nuclei which consistently show multiple indentations or deep folds, and two cell-matrix adhesion macromolecules (vinculin and fibronectin) [24, 25].

Simplistically, the myofibroblast differentiation process can be described as a positive feedback loop that requires the concurrent action of at least three factors: the cytokine transforming growth factor (TGF-β1), the presence of mechanical tension, and the ED-A splice variant of cellular fibronectin (an extracellular matrix component) [14], (Fig. 1.1). Fibroblasts respond to the

development of mechanical tension by upregulating TGF-β1 production and expressing the α-SMA isoform; in turn, α-SMA expression strengthens the contractile apparatus and increases tension development [14].

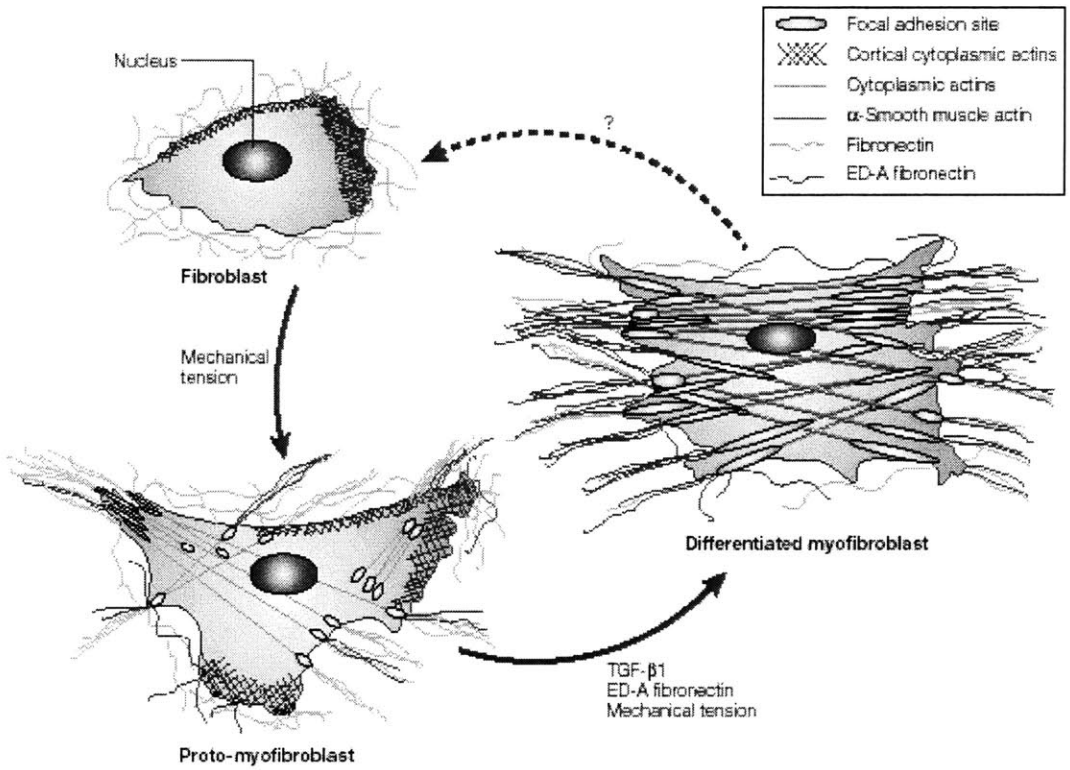

Figure 1.1: The two-stage model of myofibroblast differentiation. *In vivo*, fibroblasts have a quiescent phenotype and do not express stress fibers or focal adhesions with the extracellular matrix (ECM). Mechanical tension prompts differentiation into proto-myofibroblasts, which form cytoplasmic actin-containing stress fibers terminating in fibronexus adhesion complexes. Proto-myofibroblasts express the ED-A splice variant of cellular fibronectin and are capable of generating contractile force. Transforming growth factor β 1 (TGF-β1) increases the expression of ED-A fibronectin. Both factors, in the presence of mechanical stress, promote the modulation of proto-myofibroblasts into differentiated myofibroblasts that are characterized by *de novo* expression of α-smooth muscle actin in more extensively developed stress fibers and by large fibronexus adhesion complexes (*in vivo*) or supermature focal adhesions (*in vitro*). Functionally, differentiated myofibroblasts generate greater contractile force than proto-myofibroblasts and exhibit a higher level of organization of extracellular fibronectin into fibrils. (Reproduced from *Tomasek JJ et al. Nat Rev Mol Cell Biol. 2002)*

1.3 Mechanism of Scaffold Regenerative Activity: Control of Contraction

In skin wounds, the mechanism of induced regeneration has been elucidated through careful modulation of the structural properties of extracellular matrix (ECM) analogs that impart contraction blocking activity (Fig. 1.2). ECM analogs that actively block contraction in skin wounds (and induce regeneration) have structural properties that accomplish three main processes: 1) inhibition of TGF-β synthesis [94], leading to downregulation of myofibroblast recruitment

following severe injury; 2) blocking orientation of myofibroblast (MFB) axes in the plane of the defect where macroscopic contraction is observed and 3) ensuring that the DRT's contraction blocking properties persist for the duration of the interim myofibroblast contractile response but not so long as to interfere with key regenerative processes.

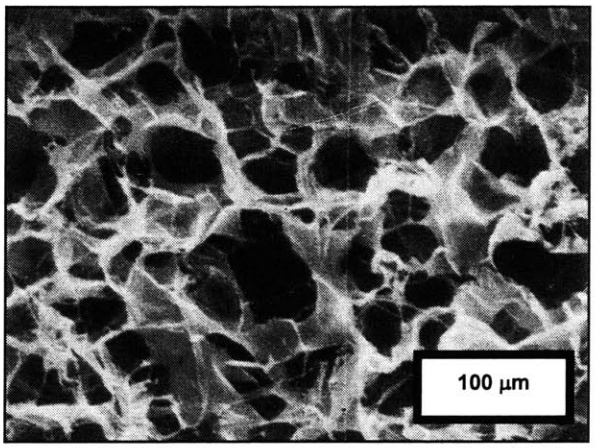

Figure 1.2: Microarchitecture of Collagen-glycosaminoglycan (CG) matrix A scaffold that has induced regeneration of the dermis in animals and humans. Composition: graft copolymer of type I collagen and chondroitin 6-sulfate. Scanning electron micrograph. Pore channel orientation is almost completely random. Average pore diameter, 80 µm.[1].

1) *Downregulation of TGF-β synthesis.* The quaternary structure of collagen fibers is a requirement for the aggregation of platelets, an early component of the wound response. Platelet aggregation initiates a cascade of events that include the release of the cytokine TGF-β1, one of the main inductors of the myofibroblast phenotype. Collagen fibers in the DRT maintain their tertiary (triple helical) structure but are practically free of banding. In this manner the DRT disrupts platelet aggregation within the defect, reducing production of TGF-β1, and the recruitment of contractile myofibroblasts to the wound site [26].

2) *Blocking orientation of MFB axes in the plane of the wound.* Contraction blocking requires extensive MFB binding onto a sufficiently large scaffold surface by specific integrin-ligand interactions. When other structural properties are held constant, a scaffold's ligand density increases with decreasing average pore size (the specific surface area of the scaffold available for attachment is increased). An appropriate ligand density is necessary to disrupt extensive MFB-ECM binding responsible for the onset of macroscopic contraction in skin wounds.

When myofibroblasts bind to specific DRT integrins that are distributed evenly in a three-dimensional, interconnecting porous network, the axes of their contractile apparatus becomes disoriented. At the cellular level, the randomized configuration of the preferential contractile axes that individual myofibroblasts adopt in the presence of DRT approximately cancels the macroscopic mechanical forces that lead to two-dimensional contraction and scar synthesis in ungrafted skin wounds. When the pore diameter of DRT is increased much beyond the level of 120 μm, the effective DRT ligand density drops to a value that does not provide sufficient binding of myofibroblasts and the contraction-blocking activity of the scaffold is lost [1, 26, 27]. Similarly, a minimal average pore size exists that is necessary to ensure MFB migration inside the scaffold. If the pore size is too small, MFB will not infiltrate the scaffold, MFB-DRT ligand bonds will not be formed, and MFB contractile activity will not be cancelled. [28]. Experimentally, the highly linear orientation of myofibroblast axes that is characteristic of the macroscopic contractile response in ungrafted skin wounds is negligible in the presence of DRT [28].

3) *Duration of DRT in an undegraded state over the entire contraction process.* In its optimal configuration, the DRT accomplishes *isomorphous tissue replacement*, in which the regenerate (dermis) is synthesized at a rate which is of the same order as the rate of degradation of the DRT. The scaffold must persist in an undegraded (insoluble) state over a period that matches the length of the contraction process in skin wounds, thereby ensuring that TGF-β1 synthesis is downregulated and MFB axes are disoriented and macroscopic contraction is blocked. The optimal half-life of degradation (t_b) for DRT *in vivo* is 14 days, roughly matching the irreversible contraction response in ungrafted wounds (t_h). When the scaffold degraded at a slower rate ($t_b >> 14$ days), the persisting DRT interfered with synthesis of the regenerate and scar formed around the scaffold. When the half-life of the DRT was significantly lower than the half-life of the contractile response ($t_b << 14$ days) the DRT had little effect on blocking contraction or scar synthesis and regeneration was not observed [29].

In summary, DRT dramatically blocks contraction while inducing skin regeneration (Fig. 1.3). Scaffolds that are close in structure to DRT but do not block contraction, do not induce regeneration. There is evidence that DRT prevents recruitment of MFB and formation of oriented structures of MFB, two processes that characterize spontaneous healing in the adult mammal, over the duration of the normal contraction process.

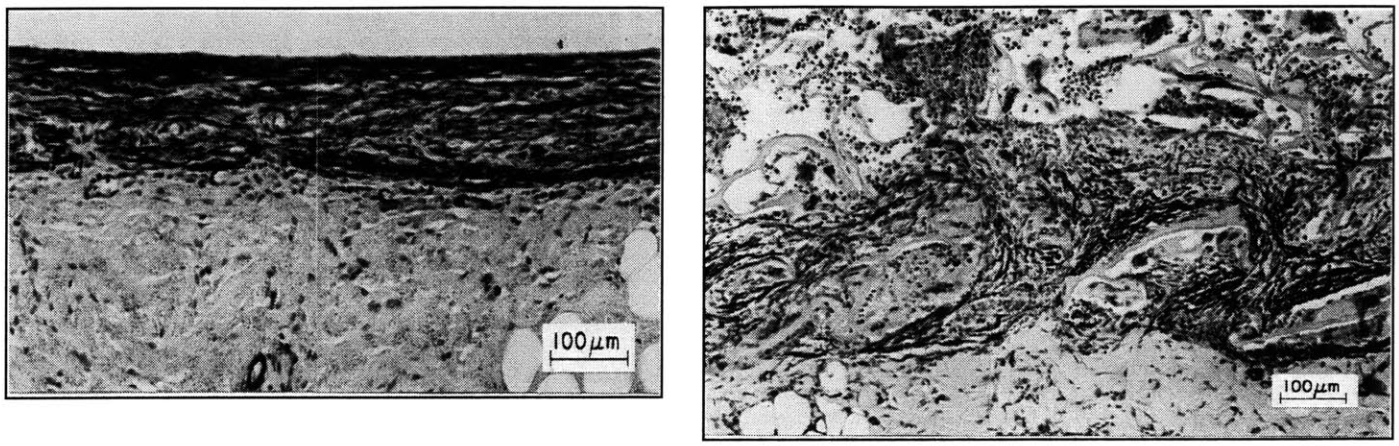

Figure 1.3: Scaffolds impart contraction-blocking by control of myofibroblast envrionment. The effect of the active scaffold (shown in Fig. 1.2) on myofibroblast organization inside wound. Myofibroblasts (dark grey) were observed inside a full-thickness skin wound in the guinea pig model 10 days after injury. *(Left)* Contraction is proceeding vigorously in this untreated skin wound (control). A thick, continuous myofibroblast layer is present at the surface of the skin wound. *(Right)* Contraction has been blocked in this treated skin wound. Myofibroblasts are dispersed inside the scaffold 10 days after injury; cell continuity is practically absent and the axes of contractile cells are almost randomly arranged in the space of the wound. Stained with monoclonal antibody against α-smooth muscle actin. Scale bar: ~ 100 μm. (Troxel, 1994.)

1.4 Intracellular Pathways Leading to Contraction

The ECM analogs described above impart contraction-blocking activity primarily by controlling the local environment of contractile cells. Increasingly, the complex inflammatory response of the adult mammal to injury is elucidated by on-going research at the cellular and molecular level. This work has shed meaningful light on the intracellular pathways that lead to expression of the contractile phenotype and force generation in connective tissue cells. Pharmacological inhibitors of various components of these pathways have been developed with varying degrees of specificity. In addition to serving as important diagnostic tools for further probing these complex processes, these inhibitors have potential clinical benefit as contraction blocking agents in studies of induced regeneration.

Cellular behavior results from a complex interaction of both mechanical and biochemical factors. The Rho GTPases have been identified as important molecular switches that play a major role in the modulation of many cellular processes including cell migration, actomyosin contractility, and cell differentiation in response to mechanical forces and other agonists including TGF-β1 [30, 31].

1.4.1 Rho GTPases

The Rho GTPases are signaling proteins that are essential to a number of cellular processes, notably the regulation of actin cytoskeleton dynamics and actomyosin contractility [32]. Three main classes of Rho GTPases are thought to be involved in the regulation of these cellular activities: Rho, Rac, and Cdc42.

Both the extending and contracting forces of a migrating cell are regulated by Rho-family GTPases [32]. These forces are necessary for cell locomotion and other cell processes, including the remodeling of the extracellular matrix (ECM) that occurs in tissue differentiation and wound healing. The G proteins Rac and Rho have been identified as key regulators of cellular morphology in three-dimensional matrices. Rac stimulates cell protrusion while Rho inhibits protrusion and stimulates contraction.

The leading edge extension of the cellular surface is driven by the Rho-family GTPases Rac1 and Cdc42 through actin polymerization. Rho kinase (ROK/RhoK/ROCK, called ROCK in this paper) has two isoforms (ROCKI and ROCKII). In non-muscle cells ROCK regulates several functions, notably actin-cytoskeleton assembly and cell contractility. Specifically, ROCK isoforms play roles in mediating the formation of RhoA induced stress fibers and focal adhesions through effects on phosphorylation of MLC and actomyosin contractility.

1.4.2 Contraction Overview

Many processes in the body depend on actomyosin contractility, including cell migration and stress fiber formation[30]. Myosin II is a major cytoskeletal protein in muscle and nonmuscle cells that is responsible for converting the chemical energy of ATP into the mechanical energy of contraction. Originally, myosin-mediated contraction was thought to be regulated by a cytostolic increase in Ca2+ according to traditional smooth muscle model of Ca^{2+} coupled contraction. Within the last 10 years, Ca2+-independent myosin II motor pathways were elucidated.

The current consensus is that smooth muscle contraction arises from the combination of two major pathways: an initial Ca^{2+}-calmodulin interaction to stimulate an initial rapid contraction via phosphorylation of the myosin light chain (MLC) and a sustained level of phosphorylated MLC due to inhibiting the action of myosin phosphatase (dephosphorylation of the MLC) by the RhoA / Rho kinase (ROCK) pathway, leading to maintained force generation [33].

Numerous non-muscle cell types (such as fibroblasts in wound beds) exhibit the ability to generate and sustain contractile forces for an extended period of time. Recent work suggests that

this force is generated by stress fibers composed of bundles of actin microfilaments, non-muscle myosin and, in the case of the differentiated myofibroblast, both E-DA fibronectin and α-SM actin and that this isometric tension is regulated by inhibition of myosin phosphatase by ROCK. [13].

Briefly, ROCK II mediates stress fiber formation by phosphorylating the MBA binding site

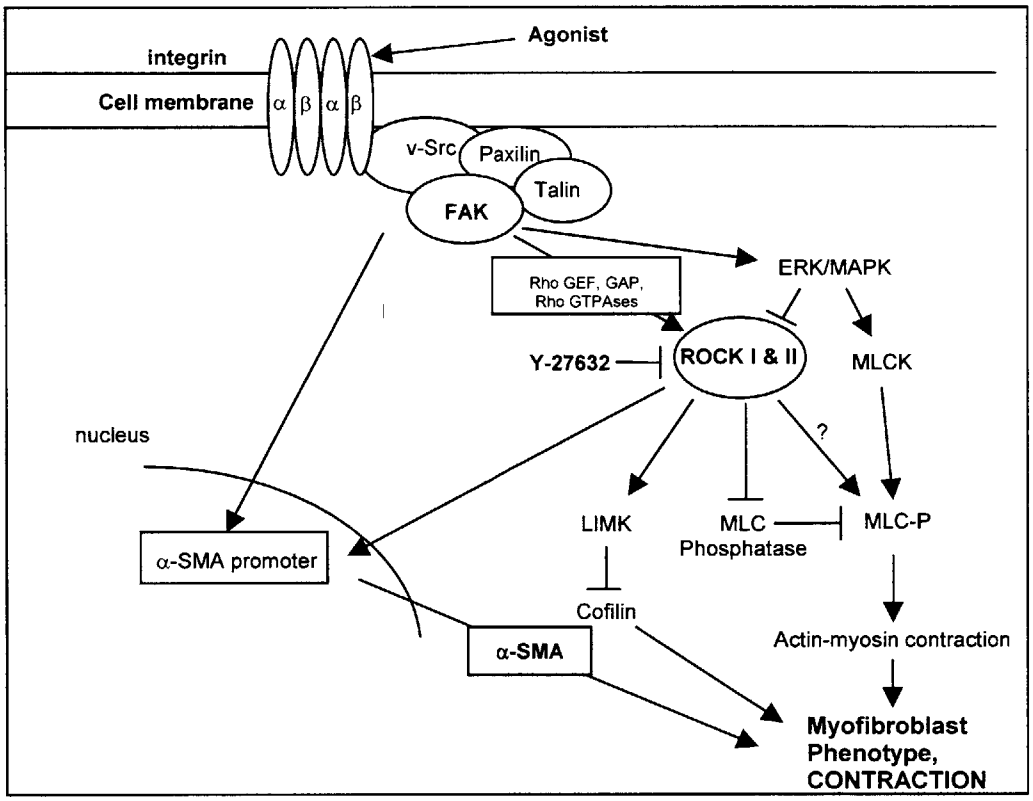

Figure 1.4: Pathways leading to synthesis of α-smooth muscle actin (α-SMA). Two agonists (top) are widely recognized: mechanical tension and TGF-β1 [2]. The pathway is a modification of pathways described in [3] and [4].

of MLC phosphatase, inhibiting its activity and leading to increased MLC phosphorylation [32]. The result is increased binding of actin as well as actin-induced ATPase activity of myosin II, ultimately leading to contraction. Because myosin is effective at crosslinking F-actin, enhanced myosin-actin binding leads to formation of F-actin into stress fibers and focal adhesions (FAs) [30].

The phosphorylation of the motor protein myosin II at the MLC_{20} (regulatory chain) has been elucidated as a key role in regulating actomyosin contractility in nonmuscle cells [34].

1.4.3 Inhibition of ROCK and Contraction

In response to external tension, fibroblasts exert sustained isometric force on their surrounding environment via a Rho/Rho-kinase (ROCK)-mediated, actomyosin contractile

apparatus. [21-23, 35, 36]. This three-dimensional, transcellular structure consists of stress fiber bundles made up of actin microfilaments, non-muscle myosin and, in the case of the differentiated myofibroblast, both E-DA fibronectin and α-SM actin [24, 25]. Through the inhibitory phosphorylation of myosin phosphatase [37], ROCK promotes myosin light-chain (MLC) phosphorylation by MLC kinase (MLCK). The resultant increase in myosin filament assembly and actin-activated myosin ATPase activity lead to sustained contraction [3], (Fig 1.4). In addition to MLC, Rho-ROCK activation of other substrates including LIM kinase (LIMK), cofilin, mDia and PIP4-5 kinase contributes to actin polymerization and stress fiber formation [38-41].

The crucial role of the downstream effector Rho kinase (ROCK) in cell-mediated contraction in response to various agonists makes it an attractive target for pharmacological inhibition. Treatment of fibroblasts and other non-muscle cells cultured in 3-D collagen lattices with Y-27632, (R)-(+)-*trans*-4-(1-aminoethyl)-N-(4-pyridyl) cyclohexanecarboxamide dihydrochloride, a specific inhibitor of the Rho-associated coiled-coil forming protein serine/threonine kinase (ROCK) family of protein kinases [42] leads to relaxation of matrix stress and prevention of myofibroblast morphology and focal adhesion maturation. Specifically, in a reversible and dose-dependent manner, Y-27632 treatment abrogates stress fibers [43-45], significantly reduces α-SMA expression [43, 45, 46], and inhibits contractile force generation measured using a stress-relaxed collagen lattice model [46, 47], an isometric culture force monitor [48, 49] and finite element modeling analysis [44]. In addition, several studies suggest the absence of toxicity or short-term side effects from Y-27632 use in animal models for the treatment of hypertension and liver fibrosis [50-53].

1.5 Methodology

1.5.1 Contraction Assay

A free-floating contraction assay was used to evaluate the effects of pharmacological inhibitors on the contractile behavior of fibroblasts *in vitro*. Free-floating three-dimensional substrates have been used widely as assays for contraction and global matrix remodeling by various connective tissue cells *in vitro* [54].

The half-life of the macroscopic contraction in ungrafted, full-thickness skin wounds is approximately 14 days (roughly matching the optimal half-life of degradation for DRT) [1]. If utilized in an *in vivo* study of induced regeneration, a reversible pharmacological inhibitor of contraction (such as those investigated in this preliminary work) would likely need to be administered over the duration of this period of time to ensure a significant contraction-blocking effect. Therefore, it was deemed important to evaluate the effects of prospective inhibitors on cellular contractile behavior for the extended period during which myofibroblast contraction occurs. Free-floating contraction experiments allow investigation of contraction and global matrix remodeling over longer time periods than isometric culture force monitors (CFMs). Replenishing cell culture medium and agonists can be done in a manner that minimally disrupts the culture conditions. The use of a culture force monitor (CFM) limits the duration of the test to two-three days, the maximum time that cells will behave normally without replacing culture medium.

1.5.2 Choice of Substrate

Collagen-GAG (CG) matrices were used as the substrate for all contraction experiments. These highly porous, three-dimensional scaffolds are prepared by a co-precipitation, lyophilization technique described in detail later. Collagen scaffolds are preferred to two-dimensional substrates as they more closely mimic the complex three-dimensional network of extracellular matrix molecules and biology of the fibroblast *in vivo* environment [55].

Importantly, collagen-GAG copolymers are effective templates for regeneration of the dermis, peripheral nerve, and conjunctiva and show promise in cartilage repair studies [1]. The use of these ECM analogs has been linked to partial regeneration of the above organs, elimination of scar tissue, and a clear contraction-blocking ability. Furthermore, these matrices are widely used as substrates for the study of connective tissue cell-mediated contraction and specifically, myofibroblastic or α-SMA-mediated contraction [56-61]. *In vitro* seeding of collagen-GAG matrices

(homogeneous cylindrical disks of 8 mm diameter) with fibroblasts results in contraction of the matrices over weeks in culture.

Scaffolds prepared using this technique have been characterized previously and have been found to have a highly uniform micro architecture, Fig 1.2. The properties of the CG matrices utilized in this study (T_f = -40 deg. C, pore size = 95 μm, pore volume fraction = .995, 24 hr dehydrothermal crosslinking) closely match those of the dermal regeneration template [1] as well as CG polymers used in other free-floating contraction experiments [56-61].

1.5.3 Cell Type

The NR6WT mouse fibroblast cell line was used for all cell-mediated contraction experiments. These cells were derived from Swiss 3T3 fibroblast line (originally isolated from 17-19 day mouse embryos) lacking endogenous mouse epidermal growth factor receptors (EGFR) and transfected with complete human EGFR (WT NR6). The contractile ability of this cell type in response to various agonists has been well-documented in contraction and cell motility experiments using fibroblast-populated collagen lattices [62-71]. Studies from this laboratory suggest that the motility and adhesion behavior of these cells bears similarity to stromal fibroblasts [72],[73]. Importantly, these cells express the integrin α5β1, which is necessary for the remodeling of CG matrices by human dermal fibroblasts [74].

Fibroblasts are the natural choice for *in vitro* mechanistic studies of induced regeneration as they are the protagonist cell in the main processes of wound healing: contraction and extracellular matrix remodeling. It has been noted that primary fibroblasts are more contractile and exhibit a higher amount of global matrix remodeling activity than cell lines in three-dimensional collagen matrices. In addition, transformed cells tend to have a lower capacity for expression of α-SMA [75, 76]. However, cell lines are far less variable and sensitive to many morphological changes that arise from two-dimensional culture conditions. Expression of many cellular proteins, especially α-SMA, is influenced by both passage number and plating density [77] in cultures of primary connective tissue cells.

1.5.4 Agents

As a pre-requisite, fibroblast contraction of collagen matrices seems to require the presence of at least one of the following agonists: serum (specifically the component lyphophosphatidic acid

or LPA), transforming growth factor beta one (TGF-β1) or platelet-derived growth factor (PDGF) [55].

1.5.4.1 Transforming growth factor-beta (TGF-β1)

The growth factor TGFβ-1, as mentioned previously, is a well-recognized inductor of the myofibroblast phenotype in many types of connective tissue cells, including fibroblasts [78]. TGF-β1 has been shown to upregulate cell-mediated contraction of both collagen [79-82] and collagen-GAG (CG) matrices [61, 83, 84] by connective tissue cells.

The proliferative effects of TGF-β on fibroblasts are dose-dependent. The literature supports the use of the agonist in the range of 1 ng/ml to 5 ng/ml for maximum effect. [2, 61, 78, 85-87]. The effects of TGF-β1 on induction of the myofibroblast phenotype decrease when the agonist is removed from the culture medium, resulting in a documented decrease in expression of α-SMA. For this reason, the dosage of TGF-β1 in this study was replenished every other day.

1.5.4.2 Y-27632, a specific Rho Kinase (ROCK) inhibitor

Y-27632, (R)-(+)-*trans*-4-(1-aminoethyl)-N-(4-pyridyl) cyclohexanecarboxamide dihydrochloride, a specific inhibitor of the Rho-associated coiled-coil forming protein serine/threonine kinase (ROCK) family of protein kinases [42] leads to relaxation of matrix stress and prevention of myofibroblast morphology and focal adhesion maturation.
The majority of studies report satisfactory inhibitory effects at a concentration of 10 μM [42]. Because of the documented reversible effect of this inhibitor on stress fiber formation, the dosage in this study was replenished every other day.

1.6 Project Goals and Overview

This work was undertaken to evaluate the effect of a specific pharmacological inhibitor on the contraction of a three-dimensional collagen-glycosaminoglycan (CG) matrix over time by attached fibroblasts treated with TGF-β1, a known upregulator of fibroblast contraction and inductor of the myofibroblast phenotype. This work is a preliminary investigation to a subsequent *in vivo* study that will evaluate the relationship between contraction blocking using pharmacological inhibitors and induced regeneration in a peripheral nerve wound model.

Chapter 2. Methodology

2.1 Preparation of Collagen-GAG (CG) Matrices

Collagen-GAG (CG) co-polymer scaffolds were prepared using co-precipitation followed by lyophilization. A CG co-polymer suspension was prepared by mixing type I microfibrillar bovine tendon collagen (Integra Life Sciences Corp., Plainsboro NJ) and 0.05M acetic acid, with an overhead blender for 3 hours at 15,000 rpm in a refrigerant-cooled flask at a constant temperature of 4° C. The GAG component, chondroitin 6-sulfate (Sigma Aldrich Chemical Co., St. Louis MO) derived from shark cartilage, was added dropwise to the suspension halfway through the blending process. Following blending, the CG co-polymer suspension was degassed with a vacuum (P=50 mTorr). Excess CG suspension that was not immediately used to make scaffolds was stored at 4° C. CG suspension stored for more than 2 weeks was re-blended and degassed again before use.

To fabricate the scaffolds, freshly degassed CG suspension was transferred to aluminum molds with a square geometry. Bubbles found in the solution were pushed to the edge of the pan with a pipette tip. The molds were then placed in a Genesis freeze-dryer (VirTis Co., Gardiner, NY), and the temperature of the freeze-dryer shelf was ramped from room temperature to a final freezing temperature of -40° C at the constant rate of 1°C/min. The freezing step results in ice crystals surrounded by collagen and GAG fibers. In the final step of the process, these ice crystals are removed by sublimation (T = 0° C, P = 75mTorr) to yield a porous, CG scaffold.

CG scaffolds were crosslinked for 24 hours using dehydrothermal treatment (DHT) in a vacuum oven at 110° C. This process imparts both sterility and decreases degradation rate of the scaffolds. CG scaffolds were stored in a dessiccator for long term storage. The protocol for fabrication of CG matrices is described in detail in Appendix A.

2.2 Free-floating Contraction Assay

2.2.1 Cell Culture and Seeding of CG Matrices

All studies were conducted with the NR6WT mouse fibroblast line cultured in T75 (75 cm^2) flasks (VWR) with 17.0 ml of complete (serum-containing) medium consisting of Dulbecco's Modified Eagle's minimum essential medium (DMEM; Invitrogen, Carlsbad, CA), supplemented with 1% Antibiotic/Antimitotic, Invitrogen) and 10% Fetal Bovine Serum (FBS; HyClone Logan

UT, Lot # ANM20369). Cells were cultured in an incubator (37° C, 5% CO2, 95% relative humidity), and passaged before reaching 90% confluence.

NR6WT cells were obtained from the lab of Douglas Lauffenburger (MIT) at passage 29 (P29). They were amplified for 2 passages, and then frozen (-80° C, liquid nitrogen) in DMSO cell freezing media (Invitrogen, Carlsbad, CA) at a concentration of 2 million cells/ml. Prior to starting an experiment, one vial of cells was defrosted and split 1:4 for 2 passages, thus yielding 16 flasks for each experimental run. Cells used in the contraction assay were at P34. Complete cell culture, passaging, and freezing protocols appear in Appendix B.

NR6WT cells (P34) were collected by trypsinization and resuspended in complete medium at a concentration sufficient to seed 1.2E6 cells/matrix. CG disks of equal size were prepared with a dermal biopsy punch (Miltex, Inc., York, PA) of 8 mm diameter. All CG disks were cut from an identical sheet of collagen-GAG scaffold. A new biopsy punch was used for each set of 6 disks.

CG disks were placed into ultra low attachment wells (6 well plates) and hydrated with sterile Phosphate Buffered Saline (Invitrogen, Carlsbad, CA) at 37 deg. C for 30 minutes and blotted dry with pieces of sterile filter paper (approximately 20 mm x 5 mm). 20 μL of cell suspension was pipetted onto the top surface of each disk and the plates were placed in an incubator at 37 deg. C, 5 % CO_2. After 20 minutes, the disks were carefully flipped and an additional 20 μL of cell suspension pipetted onto the other side. All plates were returned to the incubator for an additional 1.5-2 hrs to facilitate cellular attachment. Following this time, 3 mL of complete media was added to all control (n=6) and non-seeded matrices (n=6).

Approximately 21% of NR6WT fibroblasts initially attach to matrices using this method. Remaining matrices received equal volumes of complete media supplemented with either 3 ng/ml TGF-β1 (Sigma-Aldrich, St. Louis, MO) (n=6) or complete media supplemented with the same dosage of TGF-β1 and 10 μM Y-27632 (CalBiochem, San Diego, CA) (n=6). Media (3.0 ml, with agonist/inhibitor as indicated above) was changed every other day. Cultures were terminated after 12 days. Unseeded disks were cultured as controls. Complete protocols for cell seeding of CG matrices and contraction experiments appear in Appendix C.

2.2.2 Measurement of Cell-Mediated Contraction (CMC)

The diameter of the unseeded matrices and cell-seeded matrices in the presence of both the agonist TGF-β1 and the inhibitor Y-27632 was measured daily for 12 days post-seeding. The

diameter of all CG disks was determined by unaided visual comparison to printed circles of a known diameter (± 0.5 mm).

Contraction was calculated as the change in matrix diameter from the day 0 value divided by the day 0 diameter. Cell-mediated contraction (CMC) is a measure of lateral strain in the substrate and was determined by subtracting the contraction of the unseeded matrices from the contraction of the seeded matrices.

$$CMC = \left(\frac{OriginalDiameter - Diameter}{OriginalDiameter} \right)_{seeded} - \left(\frac{OriginalDiameter - Diameter}{OriginalDiameter} \right)_{\substack{aveage \\ unseeded}}$$

2.2.3 Matrix Digestion

At the end of the twelve day experiment all cell-seeded scaffolds were removed from culture medium, washed twice in sterile Phosphate Buffered Saline Solution (PBS) and enzymatically digested with a 2.0 U/ml solution of Dispase (Invitrogen, Carlsbad, CA) to yield a cell suspension. All CG matrices (n=6) from each of the three experimental groups (control cells, TGF-β1, and TGF-β1 + Y-27632) were digested together for 30 min. at 37 deg. C. Aliquots of the resultant cell suspension for each experimental group were mixed with Trypan blue exclusion dye (Invitrogen, Carlsbad, CA) and the number of viable cells was determined with a hemocytometer. Four counts were conducted for each experimental group (n=6 matrices). A detailed protocol for matrix digestion appears in Appendix D.

2.3 Statistical Analysis

Statistical significance was determined using analysis of variance (ANOVA) with a significance criterion of $p < 0.05$ using SigmaStat (SPSS, Chicago, IL). Curve fitting was accomplished using SigmaPlot (SPSS, Chicago, ILL). Multiple comparisons utilized the Tukey post hoc test, the most conservative test that was appropriate for the experimental conditions tested.

Chapter 3. Results

3.1 Contraction of Collagen-Glycosaminoglycan (CG) Matrices

The diameter of non-seeded control scaffolds decreased to an average of 93 % of the original diameter after 12 days. In contrast, cell-seeded constructs contracted to 84 % of the original diameter over the same time period (Fig. 1). Two-factor ANOVA revealed significant effects of both scaffold seeding of NR6WT fibroblasts ($p < 0.001$) and time in culture ($p < 0.001$) on contraction of collagen-GAG matrices.

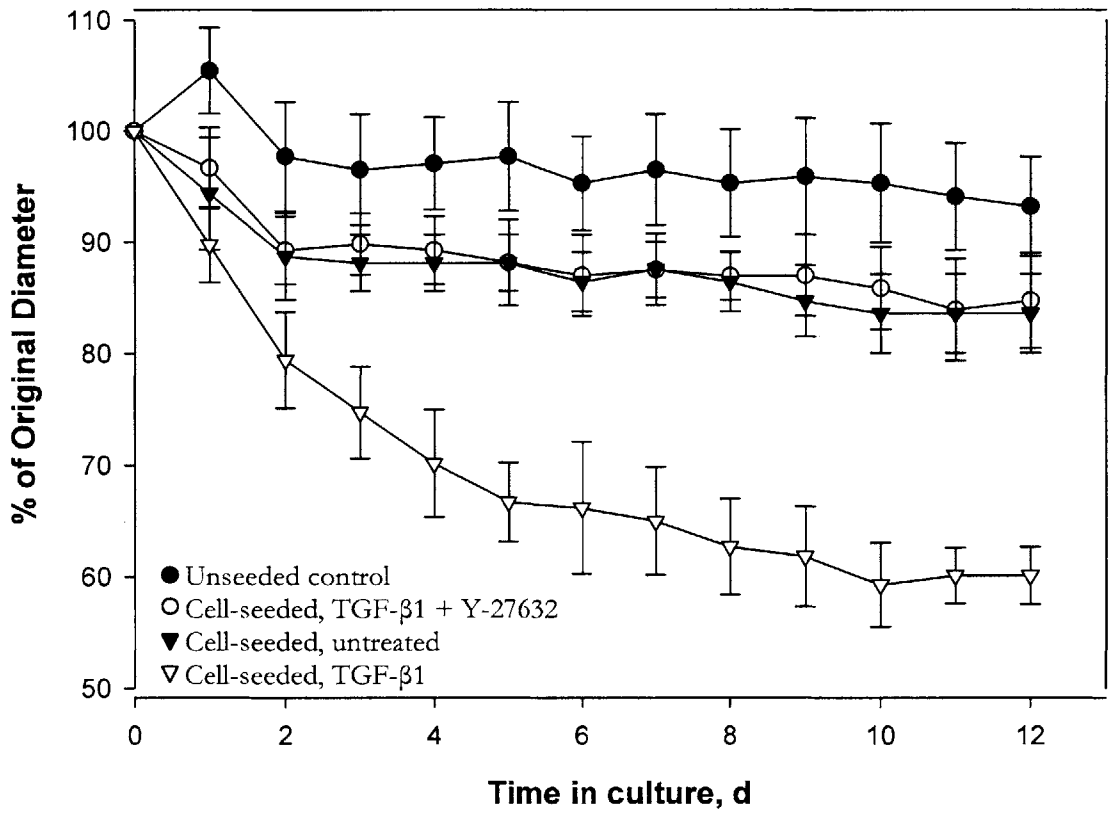

Figure. 3.1 Reduction in diameter of non-seeded control matrices, scaffolds seeded with NR6WT fibroblasts, and seeded scaffolds in treated with TGF-β1 and both TGF-β1 and the Rho kinase (ROCK) inhibitor Y-27632. Data represent means ± SD.

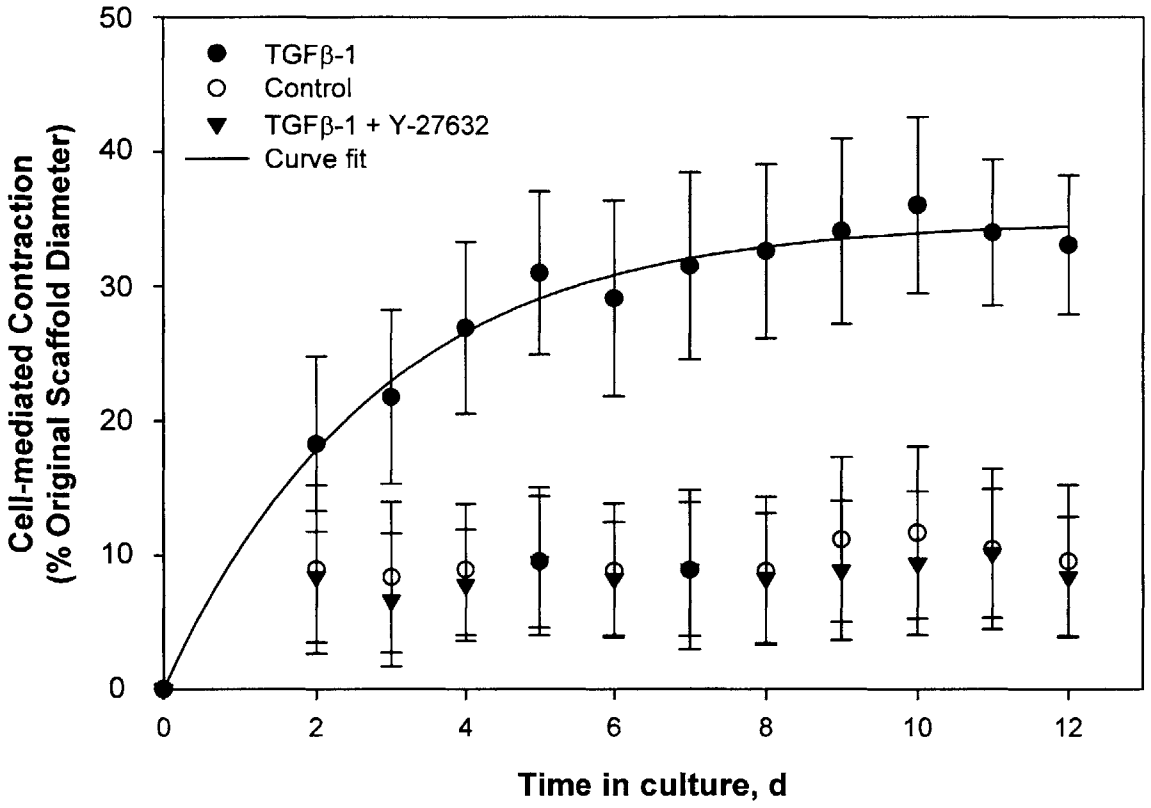

Figure. 3.2 Graph of cell-mediated contraction (CMC) as a percentage of the original diameter versus time for each treatment group. The CMC was obtained by subtracting the percentage change of the diameter of the unseeded matrix from the percentage decrease in the diameter of the cell-seeded matrix samples. Mean ± SD. Curve fit shown of the form $y = A(1 - e^{-t/\tau})$ for experimental group treated continuously with TGF-β1 ($R^2 = .98$)

3.2 Cell-mediated Contraction of CG Matrices

By day 12, the untreated (control) NR6WT fibroblasts contracted the collagen-GAG matrices (n=6) an average of 10 %, based on the original diameter of the samples (after subtracting the contracture of non-seeded matrices), Fig. 3.2.

NR6WT fibroblasts treated continuously with TGF-β1 (3 ng/ml) contracted the collagen-GAG matrices (n=6) significantly higher than control cells at all time points past day 3, approaching an average asymptotic cell-mediated contraction value of 33% by day 12 (Fig. 3.2).

Two-factor ANOVA indicates a significant effect of time ($p < 0.001$) and TGF-β1 treatment ($p < 0.001$) on cell-mediated contraction of the collagen-GAG matrices by NR6WT fibroblasts. One Way Analysis of Variance (ANOVA) with a Tukey post-hoc test showed a statistically

significant difference between day 12 values of the mean CMC of control cells and TGF-β1-treated cells ($p < 0.0001$).

Fibroblasts treated continuously with both the Rho-kinase (ROCK) inhibitor Y-27632 (10 μM) and TGF-β1 (3 ng/ml) contracted the collagen-GAG matrices (n=6) and reached an average cell-mediated contraction value of 9% by day 12 (Fig. 3.2).

Two-factor ANOVA indicates a significant effect of time ($p < 0.001$) but not of Y-27632 treatment ($p = .323$) on cell-mediated contraction of the collagen-GAG matrices by NR6WT fibroblasts. Tukey post-hoc testing did not indicate a statistically significant difference between the day 12 average CMC values of control NR6WT cells and those continuously treated with TGF-β1 + Y-27632-treated ($p = .920$). One Way ANOVA with a Tukey post-hoc test showed a statistically significant difference between the day 12 mean values of CMC for TGF-β1-treated cells and TGF-β1 + Y-27632-treated cells ($p < 0.001$).

3.3 Regression Analysis

The mean TGF-β1 cell-mediated contraction data were fit with a curve of the form $y=A(1-e^{-t/\tau})$ having an asymptote (A) of 34% of the original scaffold diameter and a time constant (τ) of 2.5 days (Fig. 3.2, $R^2 = 0.98$). The mean TGF-β1 + Y-27632 cell-mediated contraction response was fit with a curve of form $y=A(1-e^{-t/\tau})$ having an asymptote (A) of 9% of the original scaffold diameter and a time constant (t) of 1.2 days ($R^2 = 0.90$). The control cell-mediated contraction data were fit with a curve of form $y=A(1-e^{-t/\tau})$ having an asymptote (A) of 10% of the original scaffold diameter and a time constant (t) of 1.2 days, ($R^2 = 0.90$). Regression analysis shows that the time constant of contraction for TGF-β1-treated cells was twice that of control cells or cells treated with both TGF-β1 and Y-27632 (Table 3.1).

Table 3.1 Parameters for regression analysis of cell-mediated contraction (CMC)

	Asymptotic % CMC, A	τ, days	Regression, R^2
Control	10	1.2	**.90**
TGFβ-1	34	2.5	**.98**
TGFβ-1 + Y-27632	**9**	**1.2**	**.90**

3.4 Cell-mediated Contraction of CG Matrices Normalized to Cell Number

The average number of attached fibroblasts per matrix for each experimental group at the time of matrix sacrifice is shown in Table 3.2. Matrices treated with TGF-β1 continuously had

slightly more cells than control matrices. Matrices treated with both TGF-β1 and Y-27632 had roughly half the number of attached fibroblasts as control matrices.

Table 3.2 Number of attached (viable) cells at conclusion of contraction experiment (day 12) determined using Trypan exclusion dye and a hemocytometer.

	Attached Cells at Sacrifice, Day 12
Control	1.55E5
TGFβ-1	1.86E5
TGFβ-1 + Y-27632	8.65E4

Cell-mediated contraction data was normalized to cell number and showed clear effects of the agonist and inhibitor on resulting contracture. The day 12 mean values of asymptotic CMC for each experimental group were normalized to cellular content (number of viable cells at time of matrix sacrifice) to yield CMC / attached fibroblasts, expressed in %/cell (Fig. 3.3).

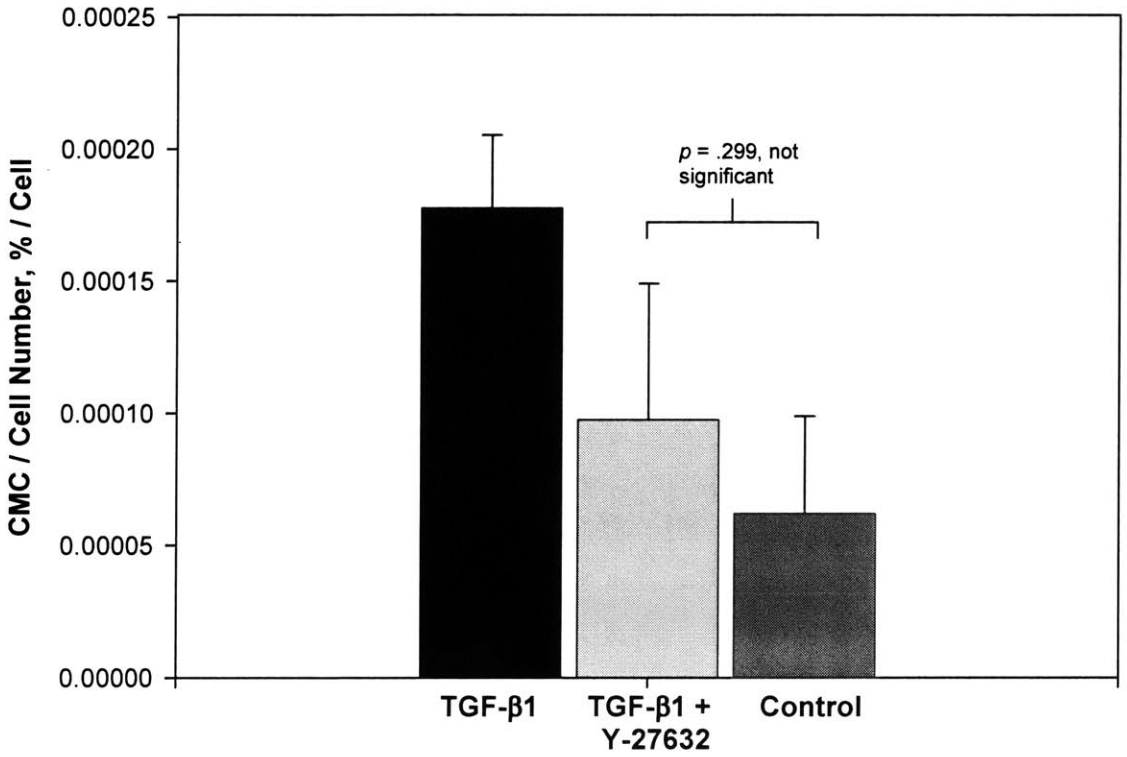

Figure. 3.3 Cell-mediated contraction, normalized to attached cell number at day 12. Addition of Y-27632 reduces TGF-β1-mediated CMC/cell number in a statistically significant manner (p =0.009). Bars represent mean values ± SD for each experimental group.

The day 12 mean value of cell-mediated contraction normalized to cell number was highest for TGF-β1-treated cells, nearly twice the magnitude of the TGF-β1 + Y-27632 group and three times that of control cells. The day 12 mean CMC normalized to cell number for the TGF-β1 + Y-27632 group was roughly 1.6 times that of the control cells. The inhibitor Y-27632 decreased the asymptotic value of CMC/cell induced by TGF-β1 treatment by nearly 50 %.

One way ANOVA with a Tukey post hoc test indicates a statistically significant difference in the day 12 asymptotic cell-mediated contraction (CMC) values normalized to cellular content between TGF-β1 treated fibroblasts and control cells ($p < 0.001$) and TGF-β1 treated fibroblasts and those treated with both TGF-β1 and Y-27632 ($p < 0.009$). No statistically significant difference between CMC/cell for control cells and TGF-β1 and Y-27632 treated cells was noted ($p = .299$).

Chapter 4. Discussion

4.1 Contraction of unseeded CG matrices

The diameter of unseeded, hydrated CG matrices decreased an average of 7 % after 12 days in free-floating culture. The tendency of unseeded, free-floating CG matrices to contract over a period of weeks in an aqueous medium has been noted in previous free-floating contraction experiments using scaffolds of identical chemical and structural properties and cross-linking treatment. While the exact mechanism of this phenomenon is unknown, it has been suggested that a likely explanation for the macroscopically observed contraction is shrinking of the pore structure due to the release of residual stresses in the CG matrices imparted during the freeze drying process by water, which is a mild plasticizer of collagen [59, 60].

4.2 Cell-mediated Contraction of CG matrices.

Seeding CG matrices with NR6WT fibroblasts resulted in a mean reduction of the diameter by 9 % after 12 days in culture (after subtracting the contractile response of unseeded matrices).

When they encounter the three-dimensional environment of a collagen matrix, fibroblasts spread, pull collagen fibrils, and extrude liquid from the matrix, contracting it [55]. The level of mechanical tension in the substrate that cells experience influences cellular behavior. The level of mechanical tension is determined by the compliance of the substrate material (modulus of elasticity) and the loading conditions of the matrix itself (free-floating or restrained). Fibroblasts adopt a quiescent, migratory phenotype in low tension environments and a more polarized, contractile phenotype in stressed matrices [55].

It has been suggested that the basal contraction of unrestrained or free-floating collagen-populated lattices (FPCL) is caused by the tractional forces generated by cell motility [2]. The FPCL has been criticized as a poor model for the study of myofibroblast differentiation and contraction as a mechanically regulated process. Similar to the early stages of wound healing, fibroblasts are known to exert tractional forces during initial integrin attachment, cell spreading and subsequent migration. The FPCL is criticized as poor model for a mechanically regulated process because it lacks the feedback mechanical signal. In the natural *in vivo* environment, tissues are tethered in a manner that cell contraction increases stress in the surrounding matrix. The absence of this mechanical signal results in a failure of resident fibroblasts in FPCLs to develop the proto-myofibroblast phenotype [2].

CG matrices are far less compliant than FPCLs, evidenced by differences in the modulus of elasticity of the two substrates [88,89] as well as observed differences in the kinetics and magnitude of lateral matrix contraction by seeded fibroblasts. In the current study of control NR6WT fibroblasts seeded in collagen-GAG matrices, there was a cell-mediated reduction in the diameter of the specimen by 9% after 12 days. These kinetics differ from those reported for fibroblast-seeded collagen gels in which as high as a 50% reduction can be found to occur within 1 day [90].

Various types of connective tissue cells, including dermal fibroblasts, have demonstrated cell-mediated contraction (and matrix deformation) and increased α-SMA expression after culture in free-floating CG matrices. Previous free-floating contraction experiments using CG matrices of identical structural and chemical properties that were seeded with connective tissue cells in a similar manner suggest that cells contract CG matrices mainly via a cell continuous layer on the surface of the sample [59, 60]. Over time pore collapse is noted at the periphery of CG matrices, suggesting contraction of the matrices is accomplished primarily by a continuous layer of cells that initially spreads on the surface of the specimen, reminiscent of the picture frame model of wound healing. Cellular morphology and pore collapse were not assayed in this study and it is not known whether NR6WT fibroblasts contracted the matrices in a similar manner. This warrants further investigation. However, it was noted that at early intermediate time points (days 1-3 post-seeding) in the experimental study, cell-continuous networks of cells were found floating in the media. These cells may have de-adhered due to full collapse of the pores on the periphery of the sample or possibly because the initial seeding density was sufficiently high to inhibit initial attachment of these cells to the CG matrix.

Aspect ratio (extent of cell elongation), the buckling of individual matrix struts, and matrix pore collapse were not assayed. This data could potentially address whether the diameter reduction of CG matrices by control NR6WT fibroblasts was due to contraction or the effects of cellular motility.

4.3 Effects of TGF-β1

The contraction of free-floating fibroblast seeded collagen-GAG matrices was significantly greater for TGF-β1 treated cells after 12 days in culture (Fig. 3.2). While the lack of mechanical feedback in free-floating matrices has caused some to doubt the ability of resident fibroblasts to express the myofibroblast phenotype, a recent study has confirmed the effect of TGF-β1 as direct agonist of fibroblast-mediated contraction and expression of α-SMA in free-floating collagen

matrices [87]. While not assayed in this study, one possible explanation for the increased contraction of CG matrices by NR6WT fibroblasts in the presence of TGF-β1 is an agonist-related increase in expression of the contractile filament α-SMA.

4.4 Cellular Viability

The initial seeding efficiency of control cells (6 hrs post seeding) was 21%, or roughly 2.7E5 fibroblasts. Seeding efficiency is determined by dividing attached fibroblasts by the total number that were pipetted onto the matrix. The number of viable cells in the matrix for each experimental group was determined at day 12, but not at intermediate data points. Prior studies using cell-seeded collagen gels indicate that cells do not proliferate in free-floating collagen gels undergoing cell-mediated contraction [91]. This observation is supported by studies utilizing several connective tissue cell types in free-floating collagen-GAG matrices [60]. Fibroblasts in floating collagen matrices adopt a quiescent phenotype and begin to enter apoptosis. In contrast, cells seem to proliferate in constrained gels, highlighting the importance of mechanical feedback to regulation of cellular behavior in the three-dimensional environment.

The average number of attached cells per matrix at day 12 varied in each of the three experimental groups. TGF-β1 treated CG matrices had a slightly higher average number of viable cells per matrix (1.9E5 cells) than control cells (1.5E5 cells). At the dosage utilized in this study TGF-β1 has a known effect on the proliferation of fibroblasts[92]. The number of attached cells at day 12 in Y-27632 treated CG matrices was roughly half that of control cells (9E4 cells). The reduced cell number after extended treatment of CG matrices with both Y-27632 + TGF-β1 warrants further investigation.

The abrogation of TGF-β1 induced contractile force with Y-27632 treatment could be due to cellular de-adhesion. Cells need an adhesive link to the extracellular matrix in order to transmit contractile force. In addition, the higher level of cell-mediated contraction induced by TGF-β1 might have resulted from a proliferative effect of the agonist on fibroblast number in these matrices. To evaluate these possibilities, asymptotic levels of cell mediated contraction were normalized by the number of fibroblasts at the termination of the contraction experiment to determine if the agonist and inhibitor had an effect on the relative CMC exerted per cell.

Differences in cell cycle, local stimuli or the extent of cell-cell contact inhibition could result in a decreased number of the attached fibroblasts actively participating in macroscopically observed matrix contraction. Direct visualization of the fibroblast aspect ratio, or the amount of cell

elongation is one method of assessing contractile activity *in vitro* [57, 58]. Aspect ratio was not assayed in this study and in the absence of this data it was assumed that all viable fibroblasts actively participated in cell-mediated contraction. As a result, the relative values reported for cell-mediated contraction (CMC) normalized to cell number (Fig. 3.3), as well as any force calculations per cell made using the data from this study are likely underestimates.

Despite this caveat, the relative magnitudes of cell-mediated contraction normalized to the attached number of fibroblasts indicate a statistically significant difference between mean values for TGF-β1 treated cells and cells treated with both TGF-β1 and Y-27632 (Fig. 3.3). In other words, the data suggest that cellular de-adhesion alone does not account for the inhibitory effect of Y-27632 on TGF-β1 stimulated cell-mediated contraction of CG matrices. A likely explanation is that the inhibitor is blocking the ability of fibroblasts to express an agonist-induced contractile phenotype and instead encouraging a switch to a more migratory one.

Cell content of matrices was determined as a global average for each experimental group rather than for each experimental sample. In future studies, cell content should be determined for each CG matrix, allowing direct conclusions to be drawn between attached cell number and force generation on a sample by sample basis.

4.5 Effects of the inhibitor Y-27632

The Rho GTPases have been implicated in TGF-β1 signaling, as well as TGF-β1-induced α-SMA expression, although the exact mechanism by which these effects are mediated remains unclear. In this study the Rho-kinase inhibitor Y-27632 significantly suppressed TGF-β1 induced contraction of CG matrices by NR6WT fibroblasts. Cell-mediated contraction was normalized to cell number indicating that these results were not solely due to cellular de-adhesion.

Studies using Swiss 3T3 cells (from which NR6WT fibroblasts are derived) indicate that the GTPase Rho is responsible for stress fiber formation. The results of the current study are consistent with previous *in vitro* work in which Y-27632 inhibited TGF-β1 induced stress fiber formation in Swiss 3T3 cells, highlighting the role of Rho in cytoskeletal remodeling and the potential therapeutic value of inhibition of Rho Kinase (ROCK) and blocking development of both the contractile apparatus and subsequent force generation in response to this factor [93].

This is the first report of Y-27632 successfully inhibiting TGF-β1-induced fibroblast-mediated contraction of a floating collagen-GAG (CG) matrix. Grinnell and Ho have observed similar results in an unrestrained collagen lattice. (unpublished results in [87]).

The observed effect of the inhibitor on contraction could have been through inhibition of the contractile filament α-SMA, although expression of this protein was not assayed in this study. Y-27632 may also have had an effect on CG matrix remodeling and more specifically, the production of type I collagen. The inhibitor has been shown to reduce the production of type I collagen mRNA in a model of rat liver fibrosis and in cultured hepatic cells [[50]. Although data on α-SMA content and type I collagen mRNA would shed additional light on the myofibroblastic character of attached cells, they were not assayed in this study.

4.6 Regression Analysis

Regression analysis revealed that NR6WT fibroblasts in all experimental groups (untreated, TGF-β1-treated, and both TGF-β1 + Y-27632 treated) approached asymptotic values of cell-mediated contraction (linear strain) during the 12 day duration of the free-floating experiment. Interestingly, the observed exponential behavior is in agreement with previous studies of macroscopic fibroblast contraction of CG matrices over the first 24 hours following cellular attachment [56-58]. In these studies, measurement of macroscopic contraction using a force transducer demonstrated that during the time when fibroblasts are attaching and spreading on CG matrices, contractile /cell data was well-modeled by a curve fit of the same type utilized in the present study for CMC/cell data [$y = A(1 - e^{-t/\tau})$]. It should be noted that the difference in the mechanical stress state between free-floating matrices and those attached to the culture force monitor, as well as the cell type used, seeding density, and CG matrices with pore structures of differing uniformity make direct comparisons difficult. In a separate study, cell-mediated contractile behavior of synovial cells in CG matrices of identical parameters exhibited exponential asymptotic behavior after a similar time in culture [60].

A previous free-floating contraction study in this laboratory utilizing dermal fibroblasts in CG matrices did not indicate the presence of an asymptotic level of cell-mediated contraction after 15 days in culture. The continued contraction observed in this study versus the asymptotic value observed in the present investigation could again be explained by the difference in cell type, cell number, or perhaps a decreased ability of the less uniform CG matrix used in the previous study to provide sufficient resistance to contraction combined with a continued decrease in resistance due to degradation with longer time in culture.

The time constants from regression analysis revealed that TGF-β1 treatment tripled the magnitude of cell-mediated contraction and doubled the time which NR6WT fibroblasts appeared

to macroscopically contract the CG matrices. Treatment with Y-27632 restored the magnitude and time constant of cell-mediated contraction to the level of control cells (10 % and 1.2 days, respectively).

4.7 Analysis of Experimental Error

A number of aspects of the experimental design could have contributed to the error associated with the diameter of CG matrices. Among the potential sources for error, the largest contribution to variation in diameter of the CG matrices is likely the blotting portion of the cell seeding procedure. This aspect of the methodology was not well standardized. Blotting was accomplished using pieces of filter paper cut to the same approximate size and the amount of time that filter paper was held in contact with matrices was not constant. Since blotting reduces the diameter of the matrix specimen, random variation in blotting time could easily have led to variation in matrix diameter.

The degree of blotting, or extraction of aqueous medium, from hydrated matrices likely affected cell seeding efficiency (attached number of fibroblasts/fibroblasts seeded) and contributed to the variation in diameter of the matrix samples in each experimental group over time. If a matrix is "under-blotted" or left in a more hydrated state prior to addition of the cell suspension with a micropipette, the effect of capillary action in drawing cells into the micro architecture of the matrix is decreased. The cell suspension could effectively sit in a puddle on top of a more hydrated matrix, decreasing the likelihood of fibroblasts to make initial integrin attachments to collagen struts necessary for initial cellular spreading and subsequent development of contractile force.

In contrast, as more and more liquid is extracted from the matrix via the filter paper, the likelihood of cells to be introduced into the matrix via capillary action is increased, likely promoting initial fibroblast attachment. However, as a hydrated CG matrix is continually blotted, the micro architecture of the matrix may become altered. Macroscopically, the hydrated matrix seems to decrease in thickness with increased blotting and likely becomes restrained laterally as it comes into contact with the underlying tissue culture plastic. It is possible that this affects the initial amount of tension in the matrix that seeded cells experience. Mechanical cues from the environment are known to affect cellular behavior including cellular spreading and whether fibroblasts adopt an initial migratory or contractile phenotype.

Additionally, while there is a degree of human error inherent to the visual determination of the diameter of the CG matrices by comparison to templates of known diameter, this error was not

quantified in this study and therefore is assumed to be zero. A more accurate, albeit destructive protocol, would be to place CG matrices in sterile PBS over a black field and digitally capture images of the diameter. Using MatLAB or Scion Image, densitometric analysis could be used to obtain a more accurate determination of the scaffold area. While this protocol requires matrices to be removed from agonist/culture conditions, digesting the matrices at these intermediate time points could facilitate further analysis of cellular viability, force per cell data, and expression of myofibroblast contractile proteins in the presence of various agonists.

As noted previously, extrapolating results obtained using 3T3-derived fibroblasts to stromal fibroblasts must be undertaken with care. The effects of TGF-β1 *in vitro* have been shown to depend on both the developmental age of fibroblasts and cell density that is treated [94, 95]. In addition, mechanical feedback is an important component of cellular behavior *in vivo* and the free-floating CG matrix assay utilized in this study may lack this key element.

Numerous factors, including platelet-derived growth factor, transforming growth factor, endothelin-1, and thrombin, seem to influence the contractile phase of wound closure and induction of the myofibroblast phenotype [14]. While the expression of α-SMA is the most widely used method of identifying myofibroblasts (its expression has been linked to an increased ability of these cells to generate force both *in vitro* and *in vivo*), whether its role in the contraction of wounds is a required one remains unclear. Depending on the clinical situation, myofibroblasts are capable of expressing other contractile proteins characteristic of smooth muscle cells [2]. Inhibition of a downstream target such as Rho-kinase (ROCK) elicits a broader effect than targeting the individual agonists of contraction or the myofibroblast phenotype described above.

Chapter 5. Conclusions and Future Work

At a dosage of 10 μM, Y-27632 significantly attenuated TGF-β1-stimulated cell-mediated contraction of free-floating CG matrices by NR6WT fibroblasts. While Y-27632 treatment also decreased the cellular content of the matrices compared to control cells, the data suggest that cellular de-adhesion alone does not account for the inhibitory effect of Y-27632 on TGF-β1 stimulated cell-mediated contraction of CG matrices. A likely explanation is that the inhibitor is blocking the ability of fibroblasts to express an agonist-induced contractile phenotype and instead encourages the development of a more migratory phenotype

. The observed effect of the inhibitor on contraction could have been mediated through inhibition of the contractile filament α-SMA, although expression of this protein was not assayed in this study. Determining the effects of Y-27632 on cellular viability, α-SMA expression, and fibroblast aspect ratio at intermediate time points in future contraction experiments would meaningfully complement cell-mediated contractile data.

The demonstrated ability of Y-27632 to inhibit TGF-β1-stimulated force generation support its use as a contraction blocking agent in a future *in vivo* study that will evaluate the relationship between contraction blocking using pharmacological inhibitors and induced regeneration in a peripheral nerve wound model.

References

1. Yannas, I.V., *Facts and theories of induced organ regeneration.* Adv Biochem Eng Biotechnol, 2005. **93**: p. 1-38.
2. Tomasek, J.J., et al., *Myofibroblasts and mechano-regulation of connective tissue remodelling.* Nat Rev Mol Cell Biol, 2002. **3**(5): p. 349-63.
3. Burridge, K. and M. Chrzanowska-Wodnicka, *Focal adhesions, contractility, and signaling.* Annu Rev Cell Dev Biol, 1996. **12**: p. 463-518.
4. Carragher, N.O. and M.C. Frame, *Focal adhesion and actin dynamics: a place where kinases and proteases meet to promote invasion.* Trends Cell Biol, 2004. **14**(5): p. 241-9.
5. Butler, C.E.a.O., D.P., *Simultaneous in vivo regeneration of neodermis, epidermis, and basement membrane.* Adv. Biochem. Engin./Biotechnol, 2005. **94**: p. 23--41.
6. Hatton, M.P.a.R., P.A.D., *Conjunctival regeneration.* Adv. Biochem. Engin./Biotechnol., 2005. **94**: p. 125--140.
7. Zhang M. and Yannas, I.V., *Peripheral nerve regeneration.* Adv. Biochem. Engin./Biotechnol, 2005. **94**: p. 67--89.
8. Mistry, A.S.a.M.A.G., *Tissue engineering for bone regeneration.* Adv. Biochem. Engin./Biotechnol, 2005. **94**(1--22).
9. Rabkin-Aikawa E., M.J.J.E., and Schoen F.J., *Heart valve regeneration.* Adv. Biochem. Engin./Biotechnol, 2005. **94**: p. 141--178.
10. Kinner B, R.C.a.M.S., *Regeneration of articular cartilage.* . Adv. Biochem. Engin./Biotechnol., 2005. **94**: p. 91--123.
11. Atala, A., *Regeneration of urologic tissues and organs.* Adv. Biochem. Engin./Biotechnol., 2005. **94**: p. 179--208.
12. Fawcett, V.P.a.J., *Spinal cord regeneration.* Adv. Biochem. Engin./Biotechnol., 2005. **94**: p. 43--66.
13. Hinz, B. and G. Gabbiani, *Mechanisms of force generation and transmission by myofibroblasts.* Curr Opin Biotechnol, 2003. **14**(5): p. 538-46.
14. Desmouliere, A., C. Chaponnier, and G. Gabbiani, *Tissue repair, contraction, and the myofibroblast.* Wound Repair Regen, 2005. **13**(1): p. 7-12.
15. Stocum, D.L., *Wound Repair, Regeneration and Artificial Tissues.* 1995, Austin, TX.: R.G. Landes Co.
16. Dahners, L.E., A.J. Banes, and K.W. Burridge, *The relationship of actin to ligament contraction.* Clin Orthop Relat Res, 1986(210): p. 246-51.
17. Ehrlich, H.P., G. Gabbiani, and P. Meda, *Cell coupling modulates the contraction of fibroblast-populated collagen lattices.* J Cell Physiol, 2000. **184**(1): p. 86-92.
18. Eyden, B., *Electron microscopy in the study of myofibroblastic lesions.* Semin Diagn Pathol, 2003. **20**(1): p. 13-24.
19. Ehrlich, H.P., et al., *Vanadate and the absence of myofibroblasts in wound contraction.* Arch Surg, 1999. **134**(5): p. 494-501.
20. Delaere, P.R., et al., *Prefabrication of composite tissue for improved tracheal reconstruction.* Ann Otol Rhinol Laryngol, 2001. **110**(9): p. 849-60.
21. Kimura, K., et al., *Regulation of myosin phosphatase by Rho and Rho-associated kinase (Rho-kinase).* Science, 1996. **273**(5272): p. 245-8.
22. Amano, M., et al., *Formation of actin stress fibers and focal adhesions enhanced by Rho-kinase.* Science, 1997. **275**(5304): p. 1308-11.

23. Hall, A., *Rho GTPases and the actin cytoskeleton.* Science, 1998. **279**(5350): p. 509-14.
24. Dugina, V., et al., *Focal adhesion features during myofibroblastic differentiation are controlled by intracellular and extracellular factors.* J Cell Sci, 2001. **114**(Pt 18): p. 3285-96.
25. Serini, G., et al., *The fibronectin domain ED-A is crucial for myofibroblastic phenotype induction by transforming growth factor-beta1.* J Cell Biol, 1998. **142**(3): p. 873-81.
26. Yannas, I.V., *Models of organ regeneration processes induced by templates.* Ann N Y Acad Sci, 1997. **831**: p. 280-93.
27. Yannas, I.V., *Studies on the biological activity of the dermal regeneration template.* Wound Repair Regen, 1998. **6**(6): p. 518-23.
28. Troxel, K., *Delay of skin wound contraction by porous collagen-GAG matrices.* 1994, Massachusetts Institute of Technology,: Cambridge, MA.
29. Yannas, I.V., et al., *Synthesis and characterization of a model extracellular matrix that induces partial regeneration of adult mammalian skin.* Proc Natl Acad Sci U S A, 1989. **86**(3): p. 933-7.
30. Chrzanowska-Wodnicka, M. and K. Burridge, *Rho-stimulated contractility drives the formation of stress fibers and focal adhesions.* J Cell Biol, 1996. **133**(6): p. 1403-15.
31. Chrzanowska-Wodnicka, M. and K. Burridge, *Rho, rac and the actin cytoskeleton.* Bioessays, 1992. **14**(11): p. 777-8.
32. Riento, K. and A.J. Ridley, *Rocks: multifunctional kinases in cell behaviour.* Nat Rev Mol Cell Biol, 2003. **4**(6): p. 446-56.
33. Webb, R.C., *Smooth muscle contraction and relaxation.* Adv Physiol Educ, 2003. **27**(1-4): p. 201-6.
34. Komatsu, S., et al., *Effects of the regulatory light chain phosphorylation of myosin II on mitosis and cytokinesis of mammalian cells.* J Biol Chem, 2000. **275**(44): p. 34512-20.
35. Katoh, K., et al., *Rho-kinase--mediated contraction of isolated stress fibers.* J Cell Biol, 2001. **153**(3): p. 569-84.
36. Katoh, K., et al., *Stress fiber organization regulated by MLCK and Rho-kinase in cultured human fibroblasts.* Am J Physiol Cell Physiol, 2001. **280**(6): p. C1669-79.
37. Kawano, Y., et al., *Phosphorylation of myosin-binding subunit (MBS) of myosin phosphatase by Rho-kinase in vivo.* J Cell Biol, 1999. **147**(5): p. 1023-38.
38. Arber, S., et al., *Regulation of actin dynamics through phosphorylation of cofilin by LIM-kinase.* Nature, 1998. **393**(6687): p. 805-9.
39. Maekawa, M., et al., *Signaling from Rho to the actin cytoskeleton through protein kinases ROCK and LIM-kinase.* Science, 1999. **285**(5429): p. 895-8.
40. Kaibuchi, K., S. Kuroda, and M. Amano, *Regulation of the cytoskeleton and cell adhesion by the Rho family GTPases in mammalian cells.* Annu Rev Biochem, 1999. **68**: p. 459-86.
41. Van Aelst, L. and C. D'Souza-Schorey, *Rho GTPases and signaling networks.* Genes Dev, 1997. **11**(18): p. 2295-322.
42. Narumiya, S., T. Ishizaki, and M. Uehata, *Use and properties of ROCK-specific inhibitor Y-27632.* Methods Enzymol, 2000. **325**: p. 273-84.
43. Patel, K., et al., *Regulation of the mesangial cell myofibroblast phenotype by actin polymerization.* J Cell Physiol, 2003. **195**(3): p. 435-45.
44. Vishwanath, M., et al., *Modulation of corneal fibroblast contractility within fibrillar collagen matrices.* Invest Ophthalmol Vis Sci, 2003. **44**(11): p. 4724-35.
45. Masamune, A., et al., *Rho kinase inhibitors block activation of pancreatic stellate cells.* Br J Pharmacol, 2003. **140**(7): p. 1292-302.
46. Zheng, Y., et al., *Involvement of rho-kinase pathway in contractile activity of rabbit RPE cells in vivo and in vitro.* Invest Ophthalmol Vis Sci, 2004. **45**(2): p. 668-74.

47. Parizi, M., E.W. Howard, and J.J. Tomasek, *Regulation of LPA-promoted myofibroblast contraction: role of Rho, myosin light chain kinase, and myosin light chain phosphatase.* Exp Cell Res, 2000. **254**(2): p. 210-20.
48. Tangkijvanich, P., et al., *Rho and p38 MAP kinase signaling pathways mediate LPA-stimulated hepatic myofibroblast migration.* J Biomed Sci, 2003. **10**(3): p. 352-8.
49. Yee, H.F., Jr., A.C. Melton, and B.N. Tran, *RhoA/rho-associated kinase mediates fibroblast contractile force generation.* Biochem Biophys Res Commun, 2001. **280**(5): p. 1340-5.
50. Tada, S., et al., *A selective ROCK inhibitor, Y27632, prevents dimethylnitrosamine-induced hepatic fibrosis in rats.* J Hepatol, 2001. **34**(4): p. 529-36.
51. Murata, T., et al., *Therapeutic significance of Y-27632, a Rho-kinase inhibitor, on the established liver fibrosis.* J Surg Res, 2003. **114**(1): p. 64-71.
52. Uehata, M., et al., *Calcium sensitization of smooth muscle mediated by a Rho-associated protein kinase in hypertension.* Nature, 1997. **389**(6654): p. 990-4.
53. Itoh, K., et al., *An essential part for Rho-associated kinase in the transcellular invasion of tumor cells.* Nat Med, 1999. **5**(2): p. 221-5.
54. Carlson, M.A. and M.T. Longaker, *The fibroblast-populated collagen matrix as a model of wound healing: a review of the evidence.* Wound Repair Regen, 2004. **12**(2): p. 134-47.
55. Grinnell, F., *Fibroblast biology in three-dimensional collagen matrices.* Trends Cell Biol, 2003. **13**(5): p. 264-9.
56. Freyman, T.M., et al., *Fibroblast contractile force is independent of the stiffness which resists the contraction.* Exp Cell Res, 2002. **272**(2): p. 153-62.
57. Freyman, T.M., et al., *Fibroblast contraction of a collagen-GAG matrix.* Biomaterials, 2001. **22**(21): p. 2883-91.
58. Freyman, T.M., et al., *Micromechanics of fibroblast contraction of a collagen-GAG matrix.* Exp Cell Res, 2001. **269**(1): p. 140-53.
59. Torres, D.S., et al., *Tendon cell contraction of collagen-GAG matrices in vitro: effect of cross-linking.* Biomaterials, 2000. **21**(15): p. 1607-19.
60. Vickers, S.M., et al., *Expression of alpha-smooth muscle actin by and contraction of cells derived from synovium.* Tissue Eng, 2004. **10**(7-8): p. 1214-23.
61. Zaleskas, J.M., et al., *Growth factor regulation of smooth muscle actin expression and contraction of human articular chondrocytes and meniscal cells in a collagen-GAG matrix.* Exp Cell Res, 2001. **270**(1): p. 21-31.
62. Reddy, C.C., A. Wells, and D.A. Lauffenburger, *Proliferative response of fibroblasts expressing internalization-deficient epidermal growth factor (EGF) receptors is altered via differential EGF depletion effect.* Biotechnol Prog, 1994. **10**(4): p. 377-84.
63. Maheshwari, G., et al., *Cell adhesion and motility depend on nanoscale RGD clustering.* J Cell Sci, 2000. **113 (Pt 10)**: p. 1677-86.
64. Glading, A., et al., *Epidermal growth factor receptor activation of calpain is required for fibroblast motility and occurs via an ERK/MAP kinase signaling pathway.* J Biol Chem, 2000. **275**(4): p. 2390-8.
65. Haugh, J.M., et al., *Internalized epidermal growth factor receptors participate in the activation of p21(ras) in fibroblasts.* J Biol Chem, 1999. **274**(48): p. 34350-60.
66. Reddy, C.C., A. Wells, and D.A. Lauffenburger, *Comparative mitogenic potencies of EGF and TGF alpha and their dependence on receptor-limitation versus ligand-limitation.* Med Biol Eng Comput, 1998. **36**(4): p. 499-507.
67. Ware, M.F., A. Wells, and D.A. Lauffenburger, *Epidermal growth factor alters fibroblast migration speed and directional persistence reciprocally and in a matrix-dependent manner.* J Cell Sci, 1998. **111 (Pt 16)**: p. 2423-32.

68. Xie, H., et al., *EGF receptor regulation of cell motility: EGF induces disassembly of focal adhesions independently of the motility-associated PLCgamma signaling pathway.* J Cell Sci, 1998. **111 (Pt 5)**: p. 615-24.
69. Reddy, C.C., A. Wells, and D.A. Lauffenburger, *Receptor-mediated effects on ligand availability influence relative mitogenic potencies of epidermal growth factor and transforming growth factor alpha.* J Cell Physiol, 1996. **166**(3): p. 512-22.
70. Koo, L.Y., et al., *Co-regulation of cell adhesion by nanoscale RGD organization and mechanical stimulus.* J Cell Sci, 2002. **115**(Pt 7): p. 1423-33.
71. Allen, F.D., et al., *Epidermal growth factor induces acute matrix contraction and subsequent calpain-modulated relaxation.* Wound Repair Regen, 2002. **10**(1): p. 67-76.
72. Shiraha, H., et al., *IP-10 inhibits epidermal growth factor-induced motility by decreasing epidermal growth factor receptor-mediated calpain activity.* J Cell Biol, 1999. **146**(1): p. 243-54.
73. Wells, A., et al., *Shaping up for shipping out: PLCgamma signaling of morphology changes in EGF-stimulated fibroblast migration.* Cell Motil Cytoskeleton, 1999. **44**(4): p. 227-33.
74. Sethi, K.K., et al., *Evidence for sequential utilization of fibronectin, vitronectin, and collagen during fibroblast-mediated collagen contraction.* Wound Repair Regen, 2002. **10**(6): p. 397-408.
75. Okamoto-Inoue, M., et al., *Alteration in expression of smooth muscle alpha-actin associated with transformation of rat 3Y1 cells.* J Cell Sci, 1990. **96 (Pt 4)**: p. 631-7.
76. Leavitt, J., et al., *Smooth muscle alpha-action is a transformation-sensitive marker for mouse NIH 3T3 and Rat-2 cells.* Nature, 1985. **316**(6031): p. 840-2.
77. Kinner, B. and M. Spector, *Smooth muscle actin expression by human articular chondrocytes and their contraction of a collagen-glycosaminoglycan matrix in vitro.* J Orthop Res, 2001. **19**(2): p. 233-41.
78. Desmouliere, A., et al., *Transforming growth factor-beta 1 induces alpha-smooth muscle actin expression in granulation tissue myofibroblasts and in quiescent and growing cultured fibroblasts.* J Cell Biol, 1993. **122**(1): p. 103-11.
79. Tingstrom, A., C.H. Heldin, and K. Rubin, *Regulation of fibroblast-mediated collagen gel contraction by platelet-derived growth factor, interleukin-1 alpha and transforming growth factor-beta 1.* J Cell Sci, 1992. **102 (Pt 2)**: p. 315-22.
80. Montesano, R. and L. Orci, *Transforming growth factor beta stimulates collagen-matrix contraction by fibroblasts: implications for wound healing.* Proc Natl Acad Sci U S A, 1988. **85**(13): p. 4894-7.
81. Fukamizu, H. and F. Grinnell, *Spatial organization of extracellular matrix and fibroblast activity: effects of serum, transforming growth factor beta, and fibronectin.* Exp Cell Res, 1990. **190**(2): p. 276-82.
82. Finesmith, T.H., K.N. Broadley, and J.M. Davidson, *Fibroblasts from wounds of different stages of repair vary in their ability to contract a collagen gel in response to growth factors.* J Cell Physiol, 1990. **144**(1): p. 99-107.
83. Kinner, B., J.M. Zaleskas, and M. Spector, *Regulation of smooth muscle actin expression and contraction in adult human mesenchymal stem cells.* Exp Cell Res, 2002. **278**(1): p. 72-83.
84. Hindman, H.B., et al., *Regulation of expression of alpha-smooth muscle actin in cells of Dupuytren's contracture.* J Bone Joint Surg Br, 2003. **85**(3): p. 448-55.
85. Vaughan, M.B., E.W. Howard, and J.J. Tomasek, *Transforming growth factor-beta1 promotes the morphological and functional differentiation of the myofibroblast.* Exp Cell Res, 2000. **257**(1): p. 180-9.
86. Miyazono, K., P. ten Dijke, and C.H. Heldin, *TGF-beta signaling by Smad proteins.* Adv Immunol, 2000. **75**: p. 115-57.
87. Grinnell, F. and C.H. Ho, *Transforming growth factor beta stimulates fibroblast-collagen matrix contraction by different mechanisms in mechanically loaded and unloaded matrices.* Exp Cell Res, 2002. **273**(2): p. 248-55.
88. Wakatsuki, T., et al., *Cell mechanics studied by a reconstituted model tissue.* Biophys J, 2000. **79**(5): p. 2353-68.

89. Harley, B. 2005.
90. Bell, E., B. Ivarsson, and C. Merrill, *Production of a tissue-like structure by contraction of collagen lattices by human fibroblasts of different proliferative potential in vitro.* Proc Natl Acad Sci U S A, 1979. **76**(3): p. 1274-8.
91. Grinnell, F., *Fibroblasts, myofibroblasts, and wound contraction.* J Cell Biol, 1994. **124**(4): p. 401-4.
92. Cordeiro, M.F., *Beyond Mitomycin: TGF-beta and wound healing.* Prog Retin Eye Res, 2002. **21**(1): p. 75-89.
93. Shen, X., et al., *The activity of guanine exchange factor NET1 is essential for transforming growth factor-beta-mediated stress fiber formation.* J Biol Chem, 2001. **276**(18): p. 15362-8.
94. Ellis, I.R. and S.L. Schor, *Differential effects of TGF-beta1 on hyaluronan synthesis by fetal and adult skin fibroblasts: implications for cell migration and wound healing.* Exp Cell Res, 1996. **228**(2): p. 326-33.
95. Ellis, I., et al., *Antagonistic effects of TGF-beta 1 and MSF on fibroblast migration and hyaluronic acid synthesis. Possible implications for dermal wound healing.* J Cell Sci, 1992. **102 (Pt 3)**: p. 447-56.

Appendix A. Collagen-Glycosaminoglycan Matrix Production

(adapted from Freyman 2001, Albers 2004, Harley 2002)

A.1 CG Co-Preciptate (Slurry) Production

Supplies

3.6 gm Type I microfibrillar bovine tendon collagen (Integra LifeSciences, Inc., Plainsboro, NJ)
2991.3ml distilled, deionized water
8.7 ml Glacial Acetic Acid
0.32 gm Chondroitin 6-sulfate (Sigma-Aldrich, St. Louis, MO)

Procedure

1. Turn on cooling system for blender (Ultra Turrax T18 Overhead blender, IKA Works, Inc., Wilmington, NC) and allow to cool to 4°C (Brinkman cooler model RC-2T, Brinkman Co., Westbury, NY).

Prepare 0.05 M acetic acid (HOAc) (pH 3.2) solution: add 8.7 ml HOAc (GlacialAcetic Acid, Mallinckrodt Chemical Co., Paris, KY) to 2991.3 ml of distilled, deionized water. This solution has a shelf life of approximately 1 week.

3. Blend 3.6 gm of microfibrillar bovine tendon collagen with 600 ml of 0.05 M acetic acid at 15,000 rpm (Setting: 3.25) for 90 minutes at 4°C.

4. Prepare chondroitin 6-sulfate solution: dissolve 0.32 gm chondroitin 6-sulfate (from shark cartilage: Cat. No. C-4384, Sigma-Aldrich Chemical Co., St. Louis, MO) in 120 ml 0.05 M acetic acid.

5. Calibrate peristaltic pump (Manostat Cassette Pump, Cat. No. 75-500-000, Manostat, New York, NY) to 120 ml per 15 minutes.

6. Add 120 ml of chondroitin 6-sulfate solution dropwise to the blending collagen dispersion over 15 minutes using the peristaltic pump, while maintaining the blender at 15,000 rpm (Setting: 3.25) and 4°C.

7. Blend slurry an additional 90 minutes at 15,000 rpm (Setting: 3.25) at 4°C.

8. Degas the slurry in a vacuum flask for 60+ minutes until bubbles are no longer present in the solution.

9. Store slurry in capped bottle at 4°C. Slurry will keep for up to four months.

10. If slurry has been stored for more than one week, reblend the slurry for fifteen minutes at 10,000rpm (Setting: 2) at 4°C and degas again.

A.2 Type I Collagen-Glycosaminoglycan Matrix Fabrication Protocol – Constant Cooling

Reference:
F.J. O'Brien, B.A. Harley, I.V. Yannas, and L.J. Gibson, "Influence of freezing-rate on pore structure in freeze-dryed collagen-GAG scaffolds," Accepted by *Biomaterials*, 2003.

Supplies

Type I collagen-glycosaminoglycan suspension (67.25ml/sheet)
5" x 5" stainless steel pan

Procedure

1. Turn on the freeze-dryer:
   » Check that the vacuum oil level is at least 2/3, the oil appears clean, and that the vacuum pump is properly vented (either outside or into a fume hood)
   » Plug the drain valve leading from the condenser and close the condenser door
   » Turn the main ***Power*** switch on
   » Turn the ***Condenser*** switch on
   » Set the ***SV*** gauge to 20°C and turn on the ***Freeze*** and ***Heat*** switches

   You need to leave approximately 60 minutes for the freeze-dryer temperature to stabilize and for the condenser to reach a cold enough temperature to continue.

2. Degas CG suspension in vacuum flask (Pressure: ~50mTorr). Degas approximately twice the necessary volume to allow appropriate removal of all air bubbles. The length of time needed to degas the suspension varies from 30min – 90min depending on the length of time the entire volume of suspension was degassed following mixing.

3. Clean the stainless steel pan with ethanol or 0.05M acetic acid and wipe the inside with Kim-Wipes to removal all dust and remaining collagen. When cleaning and handling the pan, do not touch the inside of the pan with your bare hands. Use gloves. Allow the pan to air dry.

4. Pipet 67.25ml of the CG suspension into the pan.

5. Remove an air bubbles introduced into the pan using a 200µl pipette tip. Drag the bubbles to the edge of the pan, allowing them to stick to the edge. Place the pan into the freeze-dryer.

6. Check the appropriate program is selected using the wizard controller. Press the button under ***Program X*** (X = 1 – 12) (Button #1) on the digital display. Select the appropriate program number using the ***Up*** and ***Down*** keys and then press the ***Edit*** key. Check the program following the appropriate progression. If the progression is incorrect, correct the values. Use the outer two buttons to scroll left or right through the program and the inner two keys to change the value of the selected criteria to match the program.

Program 2: Ramp to –40°C. Total time from start to sublimation: ~135 minutes
Average pore size: 95.9 ± 12.3μm.
Percent Porosity: 0.995
Specific Surface Area (S.A./Vol): 0.00748 μm^{-1}

Freezing Step	Temperature, °C	Time, min	R/H
1 (start)	20	5	H
2 ("ramping")	-40	15	R
3 ("annealing")	-40	> 60	H

Program 3: Ramp to –30°C. Total time from start to sublimation: ~105 minutes
Average pore size: 109.5 ± 18.3μm.
Percent Porosity: 0.995
Specific Surface Area (S.A./Vol): 0.00655 μm^{-1}

Freezing Step	Temperature, °C	Time, min	R/H
1 (start)	20	5	H
2 ("ramping")	-30	10	R
3 ("annealing")	-30	> 60	H

Program 4: Ramp to –20°C. Total time from start to sublimation: ~90 minutes
Average pore size: 121.0 ± 22.5μm.
Percent Porosity: 0.995
Specific Surface Area (S.A./Vol): 0.00593 μm^{-1}

Freezing Step	Temperature, °C	Time, min	R/H
1 (start)	20	5	H
2 ("ramping")	-20	10	R
3 ("annealing")	-20	> 60	H

Program 5: Ramp to –10°C. Total time from start to sublimation: ~80 minutes
Average pore size: 150.5 ± 32.1μm.
Percent Porosity: 0.995
Specific Surface Area (S.A./Vol): 0.00477 μm^{-1}

Freezing Step	Temperature, °C	Time, min	R/H
1 (start)	20	5	H
2 ("ramping")	-10	5	R
3 ("annealing")	-10	> 60	H

NOTE: In all cases, step 3 should run for 60 minutes, but it is given a longer time in case you are delayed in returning. It is acceptable for that step to run longer than 60 minutes, as you are just canceling the program after 60 minutes to start the vacuum.

7. After confirming the program, press the two middle keys on the Wizard together to cancel out of the program. Select the ***Save*** option from the menu. The Wizard screen should return to the original screen seen at start-up.

8. Turn off the ***Freeze*** and ***Heat*** buttons, turn the ***Auto*** button on, and press the ***Start*** key. The program should start running. Leave the program to run for the specified length of time.

9. At the end of the 60 minute annealing period, cancel the program. Press the middle two buttons on the wizard controller together, and then when prompted press the outer two keys. Turn off the ***Auto*** switch, then turn on the ***Freeze*** and ***Heat*** switches and set the ***SV*** to the appropriate temperature of freezing (-10, -20, -30, or –40°C).

10. Turn on the ***Vacuum*** switch. Make sure the seal on the condenser and chamber doors in tight and put pressure on the door to the condenser until a vacuum pressure registers on the pressure reading in the wizard control screen (typically ~1900mTorr).

11. When the vacuum pressure reaches below 300mTorr, raise the temperature in the ***SV*** display to 0°C. Allow the freeze-dryer to run for 17 hours at a temperature of 0°C and a pressure <300mTorr.

12. After 17 hours, raise the value of the ***SV*** control to 20°C. Wait for the chamber temperature to equilibrate to 20°C (temperature displayed in the ***PV*** display). Turn off the ***Vacuum*** switch and turn on the ***Chamber Release*** switch. Wait for the pressure to be equilibrated. Remove the pan.

13. Turn off the freeze-dryer:
    - » Turn off the ***Chamber Release*** switch
    - » Turn off the ***Freeze*** and ***Heat*** switches
    - » Turn off the ***Condenser*** Switch
    - » Turn off the ***Power*** Switch
  - » Open the condenser door, unplug the condenser drain line and place it into the drain bucket.

14. Remove the CG scaffold from the pan with gloved hands. Place the scaffold into an aluminum foil packet and store in a dessicator.

15. Wash the stainless steel pan with ethanol or 0.05M acetic acid and wipe down with Kim-Wipes to remove any portion of the scaffold that may have torn during removal.

16. Return the pan to storage.

17. Make notation on run sheet attached to the front of the freeze-drier in order to keep track of the total number of runs between oil changes. When a row is completely checked off (10 freeze-drier runs), change the oil.

A.3 Dehydrothermal Crosslinking Protocol

Procedure

1. Place collagen material in aluminum foil packet. Leave packet open at top.

2. Place packet in vacuum oven (Isotemp Model 201, Fisher Scientific, Boston, MA) at established set temperature. The following settings are for both the collagen-glycosaminoglycan (CG) matrices and for 5% collagen tubes (multiple settings possible).

Matrix	Set Temperature	Exposure Time
CG matrix	105°C	24 hours

3. Turn on vacuum. The vacuum oven should reach a final pressure of approximately -29.7 mmHg.

4. At the end of the exposure period, turn off the vacuum and cent the chamber. Open the vacuum door and immediately seal the aluminum foil bags. The matrix is now crosslinked and considered sterile, so the matrix should only be handled under sterile conditions from now on.

5. Store the matrix in a dessicator. Crosslinked matrices can remain indefinitely in a dessicator prior to testing or use.

Appendix B. Cell Culture Protocol

(adapted from Albers, 2004)

Equipment:

NAPCO 6000 Series CO_2 Incubator, set to 37°C 5% CO_2 and 95% relative humidity (VWR Scientific/PrecisionNAPCO, Winchester, VA)

Water Bath, set to 37°C

Sterile Hood, laminar flow or traditional

Inverted Cell Culture Microscope (Nikon TMS-F)

Centrifuge [set to 900RPM] (Heraeus Labofuge 400)

Materials:

5mL, 10mL, 25mL Sterile Pipettes

PipetteAid Hand mechanical pipetting device

250mL waste beaker

Supplies / Stains:

500mL Bottle DMEM (Gibco 12320-032)

5mL Antibiotic-Antimycotic [containing 10,000U/mL penicillin G sodium, 10,000μg/mL streptomycin sulfate, and 25μg/mL Fungizone] (Gibco 15240-062)

50mL Characterized Fetal Bovine Serum (Hyclone, Logan, UT)

Trypan Blue Stain (Gibco 15250-061)

Trypsin-EDTA (0.05%Trypsin) (Gibco 25300-062)

B.1 Media Preparation

1. Place all media supplies in a water bath at 37°C to thaw/warm.
2. Spray down 2x25mL and 1x5mL pipettes with 70%EtOH and place in a sterile hood.
3. When media supplies are ready, wipe down all bottles and spray with 70% EtOH before placing in sterile hood.
4. Remove 55mL of DMEM from a full sterile bottle of media and discard.
5. Add 50mL FBS and 5mL Antibiotic-Antimycotic.
6. Cap and gently swirl to mix.

B.2 Cell Feeding

1. Warm media in water bath at 37°C.
2. Spray down 2x25mL pipettes, PipetteAid, and waste beaker with 70% EtOH. Place in sterile hood.
3. When media is warm, wipe dry with paper towel and spray with EtOH before placing in sterile hood.
4. Using 25mL pipette, remove all liquid from all flasks, taking care not to scrape cells with pipette tip.
5. Replace with 17mL complete media at 37°C using a new, sterile pipette tip.

B.3 Cell Passaging

1. Warm complete media, DPBS, and 4mL Trypsin (per flask to be passaged) in water bath at 37°C.
2. Spray down 2x25mL 2x10mL, and 1x5mL pipette, PipetteAid, and waste beaker with 70% EtOH and place in sterile hood.
3. When media, PBs, and Trypsin is warm, wipe dry with paper towel and spray with EtOH before placing in sterile hood.
4. Using 25mL pipette, remove all liquid from all flasks, taking care not to scrape cells with pipette tip.
5. Add 5mL DPBS per flask and set horizontally for 30 seconds. Swirl gently to remove any remaining media from edges.
6. Remove DPBS and add 4mL Trypsin per flask.
7. Incubate for 7 minutes to facilitate detachment. (If necessary, allow cells to sit for 3-4 additional minutes if not detached.)
8. Add 6mL complete media to each flask.
9. Split each 10mL flask into four (4) new, sterile flasks, with 2mL cell suspension each.
10. Top off with 15mL additional complete media per flask and return to incubator.

B.4 Cell Counting Procedure

1. Remove 100 μL from cell suspension while maintaining sterile conditions.
2. Mix 100 μL of cell suspension with 100 μL Trypan blue. Pipette several times to mix stain and cell suspension.
3. Place cover slip on hemacytometer and pipette 10 μL of stain/cell suspension into notch.
4. Cell counts were done in all 5 boxes shown below. Average cell number per box (total number of cells counted / total boxes counted) was used in the calculation of cell quantities, as shown in the equation below. (Note: "10,000" is a volumetric multiplier used to convert from the volume above each square (0.1μL) to the "# cells / mL" quantity desired.

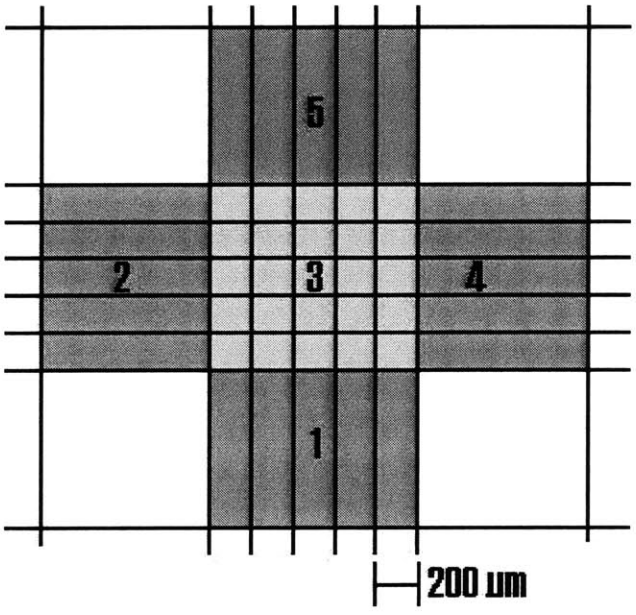

(In order to prevent double counting of cells at the junction of two or more squares, cells were counted as being in a square only if more than half of the cell was lying on either the bottom or right edge of the square in question.)

$$\#Cells = \frac{\#counted}{squares\ counted} \cdot Dilution(2) \cdot 10,000 \cdot Volume(ml)$$

1.

B.5 Cell Freezing

Fibroblasts can be stored in liquid N_2 vapor for extended periods of time. Perform procedure under sterile conditions and warm all solutions to 37°C before use.

1. Produce a cell suspension from cells at ~90% confluence using the procedure outlined in the "Cell Passaging Procedure".

2. Count cells using "Cell Counting Procedure"

3. Resuspend cells in cell freezing medium (Gibco) at a density of ~ 1 million cells/ml.

4. Distribute 1 ml to each cryovial. Ensure that cryovials are sealed.

5. Place cryovials into a styrofoam container with walls ~15 mm thick and pack container with cotton gauze. Seal with tape and place in the vapor phase of liquid N_2 dewar.

6. Wait 4 h for cell suspension to freeze and then transfer cryovials to a plastic box in the dewar racks.

Appendix C. Free-Floating Matrix Contraction

(Adapted from Freyman, 2001)

Protocol for seeding and measuring the contraction of free-floating, fibroblast-seeded, matrix disks. This is a general procedure and the number of samples and cell densities will vary depending on the required experimental parameters. All steps should be performed following cell-culture sterile protocol.

Equipment:

6-well tissue culture plates (low-attachment)
forceps
collagen-GAG matrix sheet
8.0 mm diameter dermal biopsy punch (Miltex Inc, York, PA)
Teflon® sheet
sheet with printed disks (0.5 mm)
50 ml centrifuge tubes
disposable, plastic pipettes
sterile filter paper

Solutions:

DMEM with 10% FBS (see Appendix B)
2.0 U/ml dispase solution (Invitrogen)
PBS
TGF-β1 (Sigma-Aldrich, Cat. # T7039, St. Louis, MO)
Y-27632 (CalBiochem, Cat. # 688001 , San Diego, CA)

Procedure:

1. Using the dermal biopsy punch cut out matrix disks on the Teflon sheet. Be careful not to tear the matrix while cutting.

2. Place one matrix disk in each well of the tissue culture plate. Place the 'pan side' of the matrix up for all samples. Rehydrate matrix disks by slowly pipetting 3 mL of sterile PBS (37 deg. C) evenly into the well around each matrix, without directly pipetting liquid onto the matrix surface. The matrix should hydrate slowly through absorption of PBS from the periphery of the sample.

3. Make a cell suspension following the protocol for cell passaging in Appendix B.

4. After 15 minutes of hydration, remove as much PBS as possible from each well carefully so as not to disturb the matrices.

5. Using pieces of sterile filter paper, remove residual PBS from the samples. Blot the matrices by placing the filter paper in contact with the 'puddle' surrounding the matrix taking care not to bring the filter paper into direct contact with the matrix itself. Hold the paper in contact until it is fully wetted. Repeat with an additional piece of sterile filter paper if necessary.

6. Add the cell suspension to the tube with rehydrated matrix disks. Cover the 6 well plates and place in the incubator. Wait 15 m.

7. Remove 6-well plates from the incubator and carefully flip cell-seeded matrices with forceps. Add the appropriate aliquot of cell suspension to the unseeded side of each matrix disk.

8. Cover 6-well plate and return to the incubator. Wait 1.5-2 hours.

9. Carefully add 3 ml of DMEM (alone or supplemented with agonists as described below) to each well in the same manner that PBS was added in the initial hydration step (step 2). Cell-seeded matrices should be floating (unrestrained) following addition of the full volume.

    9.a. *TGF-β1-treated samples*:

    3.5 μL of a thawed aliquot of TGF-β1 (originally diluted to a concentration of 50 μg/ml with sterile deionized H_2O) should be added to 18 mL of complete media in a 50 mL centrifuge tube to achieve a working concentration of 3 ng/ml (enough for 6 matrices).

    9.b.*TGF-β1 + Y-27632-treated samples:*

    Media should be prepared as in 9.a. with the addition of 38 μL of a thawed aliquot of Y-27632 (5 mM) to achieve a working concentration of 10 μM for the inhibitor (enough for 6 matrices).

    Change the medium (3.0 ml) and agonist/inhibitor every other day through the course of the experiment.

10. Measure the diameter of each matrix sample by comparing the disk size to printed circles of known diameter (0.5 mm increments). If the disk appears elliptical estimate the major and minor axis dimensions.

11. Repeat disk diameter measurements daily.

10. On day 12 sacrifice matrix samples for cell number determination (n=6) using scaffold digestion protocol (Appendix D).

Appendix D. CG Matrix Digestion Procedure

Solutions

Dulbecco's Phosphate Buffered Saline (DPBS) (14190-144, Gibco)
Dispase Solution [2.0 U/ml]
DPBS, Dispase (17105-041, Gibco)
Trypan Blue (15250-061, Gibco)

Procedure:

1. Place ~ 5ml DPBS in 15ml centrifuge tubes (one per sample). Warm DPBS to 37°C.

2. For each experimental group of n=6 matrices (control cells, agonist-treated, agonist + inhibitor-treated), add enough dispase powder to 12.0 ml DPBS to make a 2.0 U/ml solution. Warm to 37°C.

3. Rinse samples in warmed DPBS by dipping 2x.

4. Digest all matrices for each experimental group by placing n=6 matrices in warmed dispase solution for 20-30 min. at 37°C.

5. Using hemocytometer count cells in digest using protocol outlined in Appendix B. Be sure to note total volume of the suspension. Count 4 times, average, and divide by number of samples (n=6) for average cell content of CG matrix.